Mathematical Analysis of the Impact of Transmission-Blocking Drugs on the Population Dynamics of Malaria

Woldegebriel Assefa Woldegerima[1,*], Rachid Ouifki[1], Jacek Banasiak[1,2]

[1] Department of Mathematics and Applied Mathematics, University of Pretoria, South Africa
[2] Institute of Mathematics, Łódź University of Technology, ul.Wólczańska 215, 90-924 Łódź, Poland

[*]Correspondence: wa.woldergerima@up.ac.za ; +27 (0) 627569977

Abstract

Recently, promising clinical advances have been made in the development of antimalarial drugs that block the parasite transmission and also cures the disease and has prophylactic effects, called transmission-blocking drugs (TBDs). The aim of this paper is to develop and analyze a population level compartmental model of human-mosquito interactions that takes into account an intervention using TBDs. We do this by extending the SEIRS-SEI type model to include a class of humans who are undergoing the treatment with TBDs and a class of those who are protected because of successful treatment. Before we proceed with an analysis of the model's stability and bifurcation behaviours, we start by ensuring that the model is well-posed in a biologically feasible domain. Mathematical analysis indicates that the model exhibits a forward and backward bifurcation under certain conditions. Results from our analysis shows that the effect of treatment rate on reducing reproduction number depends on other key parameters such as the efficacy of the drug. The projections of the validated model show the benefits of using TBDs in malaria control in preventing new cases and reducing mortality. In particular, we find that treating 35% of the population of Sub-Saharan Africa with a 95% efficacious TBD from 2021 will result in approximately 82% reduction on the number of malaria deaths by 2035.

Keywords: Transmission-blocking antimalarial drug, mathematical modeling, data fitting, treatment coverage, drug efficacy, bifurcation analysis, numeral simulation

1 Introduction and Motivation

Malaria is a vector-borne infectious disease caused by the replication of protozoan parasites of the genus *Plasmodium* inside red blood cells. It can be transmitted to vertebrates, including humans of all ages, by female mosquitoes of the genus *Anopheles*, when they feed on blood. Malaria is one of the most severe public health problems worldwide, being one of the leading causes of death in many developing countries, where young children and pregnant women are most affected [70, 69]. According to the WHO malaria report (2019) [70], there were an estimated 228 million cases of malaria worldwide in 2018, resulting in around 405000 deaths. The WHO African Region carries a disproportionately high share of the global malaria burden with as much as 93% of malaria cases and 94% of malaria deaths recorded in Africa in 2018, [70].

For almost a century, several strategies and methods have been developed, at both the population and cellular levels, in an effort to control malaria transmission and spread. These range from the

non-therapeutic prevention and control measures (such as insecticide treated bed nets, indoor residual spraying and other vector control measures), to antimalarial drugs (for prophylaxis, treatment and transmission blockage) [21, 48, 71]. Nonetheless, as mentioned above, despite the efforts, malaria remains a major global health problem. One of the major challenges facing malaria control is the continuous emergence of resistance to the first line of antimalarial drugs and insecticides. Another important problem is that most of the antimalarial drugs are not active against sexual stage *P. falciparum* parasites, called gametocytes, which are responsible for the spread of malaria from person to person via mosquitoes.

Recent studies indicate that to achieve global eradication of malaria, it will be necessary to use interventions that block the transmission of the *Plasmodium* from humans to mosquitoes and back, [21]. One way of doing this is to directly target the parasite using transmission-blocking interventions (TBIs). These can be broadly classified as transmission-blocking drugs (TBDs) or transmission-blocking vaccines (TBVs), [21]. Both approaches intend to stop the transmission of gametocytes from humans to mosquitoes in one of the ways described below.

For the treatment of uncomplicated malaria, WHO recommends the use of artemisinin-based drugs that have the capacity of acting against both asexual blood stage and the gametocyte stages of the parasite, [4, 9, 15, 71]. However, malaria parasites have showed resistance to the artemisinins, characterized by a reduced rate of parasite clearance and thus allowing for their partial transmission, hence more sophisticated drugs should be used. We note that each antimalarial drug has different attributes, including killing efficacy against the parasites, duration of effect, gametocytocidal activity, mosquitocidal activity, liver-stage activity (especially, for *Plasmodium vivax*), dosing schedule and toxicity, [58], according to which they can be classified, [6, 56]. For example, gametocidal antimalarial drugs (which form a large group of TBDs) are designed to inhibit the development of the sexual forms of the parasite in blood and block its transmission to mosquitoes, [61]. Thus, as indicated in [58], a key to the optimal drug design for malaria elimination and control is the integration of the results obtained from analysis of mathematical models for the human-mosquito population level transmission dynamics of malaria with those coming from the cellular-level pharmacokinetics and pharmacodynamic (PK/PD) models. In particular, the population level models can suggest the deployment strategy and quantify effective treatment coverage and endemicity-level.

Over the past century, many population level malaria models with various levels of complexity, not considering, however, the TBDs, have been developed and analysed by many authors. The first compartmental differential equation models of malaria as a host-vector disease were developed by Ross in [55] and later Macdonald [42]. Their conclusions that the endemicity of malaria is most sensitive to the changes in the mosquito survival rate and that malaria can persist in if the mosquito population is sufficiently large, as well as the relation of the prevalence of infections to the so-called basic reproductive number, are still fundamental in malaria research. Several authors have extended the Ross-Macdonald model in various directions, see e.g. [3, 5, 16, 24, 46, 49, 67] and references therein. Recently, the climate change has become an important aspect in malaria modelling, see e.g. [26, 44, 49, 74]. Some other mathematical models include the age-structure, see e.g. [7, 25, 31], and the treatment using the usual antimalarial drugs [20, 47].

As mentioned above, the paper considers special types of antimalarial drugs, called TBDs, that are designed to be administered to the humans, so that they either target the parasite within the human-host or during the parasite's developmental stages within the mosquito after ingested during the blood meal. In general, according to [57, 66], TBDs can be classified as follows.

(i) **Drugs targeting the malaria parasite within the human-host**. This category includes: (a) drugs killing asexual stages of the parasite so that their progression to gametocytes is stopped/reduced; (b) drugs reducing the commitment of asexual parasites to gametocytes within the human cycle; (c) drugs directly targeting immature and mature gametocytes within the human; (d) drugs providing chemo-prophylaxis by directly acting on sporozoites, hence halting the infection.

(ii) **Drugs targeting the parasite in the vector**. This category includes drugs that target the developmental stages (ingested gametocytes in the midgut of vector, male and female gametes, zygote, ookinete, oocyst and the sporozoites) of the parasite.

(ii) **Drugs targeting the vector itself**. These are special drugs, known as *endectocides* [57, 66], that are administered to humans and intended to kill the mosquito when ingested at a blood meal.

Commonly used antimalarial drugs such as primaquine and artemisinin have gametocidal activity for *Plasmodium falciparum* [9, 51]. Primaquine (PQ), methylene blue (MB) and atovaquone (ATQ) are clinically approved antimalarial that have transmission-blocking properties, [9, 21]. The gametocytocidal activity of compounds is known to differ, with most current artemisinin compounds having high efficacy against the early stages (stages $I - IV$) of gametocyte, however, some compounds, including primaquine and tafenoquine, attack the later, mature, stage V, [58]. While these transmission-blocking properties of common drugs have been known for some time, it was realized that for eradication of malaria it was necessary to develop drugs specifically designed to completely block *Plasmodium* parasites transmission, [4].

There have been many promising clinical advances in the discovery of TBDs, see [4, 9, 21, 66], but to the authors' knowledge, there have been few attempts to model the impact of TBDs on the malaria transmission rates and the spread of the disease at the population level, which depend strongly on the macroscopic variables such as the deployment strategy, treatment coverage, efficacy of the drugs used and the endemicity levels. We note the research by Bretscher et al. (2017), [12], where a mathematical model was used to estimate the transmission reduction that can be achieved by using drugs of varying chemo-prophylactic or transmission-blocking activity.

The aim of this paper is to fill this gap by investigating the impact of the treatment with TBDs on malaria dynamics. To do so, we formulate a mathematical model for the human-mosquito population level transmission dynamics of malaria that considers a treatment using TBDs and provide its qualitative analysis. To get quantitative results, we fit the proposed model to the data from the Institute of Health Metrics and Evaluation (IHME)-Global Burden of Disease (GBD) for Sub-Saharan Africa, [54] by using the "lmfit" package, which is a non-linear least-squares minimization and curve-fitting package in Python, [45]. We believe that our model can provide important mathematical and epidemiological insights into the effects of TBDs on the malaria transmission rates and, thanks to its flexibility, it can help in designing and implementation of the treatment in a best way for the disease control and elimination.

The paper is organized as follows. In Section 2, we formulate the model and in Section 3 we present its mathematical analysis. In particular, in Subsection 3.3 we study the dependence of the control reproduction number on the treatment coverage rate and the efficacy of the TBD and in Subsection 3.5 we carry out a rigorous study of the existence and the number of endemic equilibria and a possibility for occurrence of the backward bifurcation. The mathematical analysis and obtained results are validated by fitting the model into real data in Section 4.

2 Model Formulation

We use the standard deterministic malaria disease transmission model with an SEIRS structure for humans and an SEI structure for mosquitoes, as introduced in [16, 19, 46], augmented by the compartments of individuals who are under treatment with TBDs and those are successfully treated and protected.

2.1 Model's assumptions and variables

The total human population N_h is divided into six classes. In addition to the standard susceptible S_h, exposed E_h, infectious I_h and naturally recovered with immunity R_h classes, we introduce two more classes, T_h for individuals who undergo the treatment with TBDs and P_h for those who were successfully treated, cured and are protected, so that they are noninfectious. In short, the R_h class consists of those human individuals who recovered and are immunized due to natural (innate or adaptive) immunity but can be still infective to mosquitoes. On the other hand, the individuals in the P_h class have undergone the treatment with a TBD and are cured and protected; they do not transmit gametocytes to mosquitoes. At any time t, the total human population is $N_h(t) = S_h(t) + E_h(t) + I_h(t) + T_h(t) + R_h(t) + P_h(t)$.

People enter the susceptible class either through birth (at a constant total birth rate Π_h) or after recovering from the disease, at a per capita rate ρ_h. They are assumed to die naturally at a per capita rate μ_h or move to the exposed class if they are bitten by an infectious mosquito and the sporozoites are passed on to them. The rate of infections in the susceptible human population is assumed to be given by $\Lambda_{vh} = \beta_{vh} b I_v S_h / N_h$, where b is the average mosquito biting rate and β_{vh} is the probability that a bite by an infectious mosquito on a susceptible human leads to an infection. We assumed that the exposed mosquitoes do not transmit malaria to humans due to the parasite extrinsic incubation period which is temperature dependent and, e.g. for *P. falciparum*, ranges from 10 to 14 days. [41]. On the other hand, though the incubation period of malaria in humans in most cases varies from 7 to 30 days, the exposed individuals are infective to mosquitoes. As follows from [41], the gametocytes (the transmissible stage of *Plasmodium*), are produced by a small fraction of merozoites that differentiate into them upon entering the red blood cells, although gametocytes of *P. vivax*, *P. ovale* and *P. malariae* can also arise from emerging liver stage merozoites. This implies that, in the latter cases, the individuals also can transmit to mosquitoes during the pre-erythrocyte stage. Furthermore, the *P. falciparum* gametocytes may linger in peripheral blood up to several weeks after an asexual parasite infection has been cleared (whether by natural immunity or by drugs) [41] so that after certain period of time one may get a reinfection by other infectious mosquitoes bite, but one can still can transmit due to the previous infection. To include this possibility in our model and give it more flexibility, we introduced a parameter $\zeta \in [0, 1)$,.

Exposed individuals either die at the rate μ_h or move to the infectious class at rate ν_h. Infectious individuals either die at a rate $\mu_h + \delta_h$, recover at a rate γ_h or start treatment with a TBD and move to the T_h class (at a rate α_h). Recovered individuals are assumed to die at a rate μ_h or gradually lose their immunity and move to the susceptible class at a rate ρ_h. Concerning people undergoing the treatment, they are assumed retain some lower level of infectiveness and can be successfully treated and move to the protected class at a rate $\psi_1(p_e)$ (which is assumed to be increasing with the drug's efficacy p_e), move back to the infectious class I_h (at a rate $q_h\psi_2(p_e)$, where ψ_2 is assumed to be decreasing with p_e), recover and move to R_h at rate $(1 - q_h)\psi_2(p_e)$, or die at the rate μ_h. Here, q_h and $1 - q_h$ are the probabilities where individuals in T_h class move back to I_h class and R_h class, respectively. Individuals in the protected class P_h either die at the rate μ_h or lose their protection and move back to the susceptible class at a rate ϑ.

The total *Anopheles* female mosquito population N_v is divided into three classes, susceptibles S_h, exposed E_h and infectious I_h. So, at time t, the total mosquito population is $N_v(t) = S_v(t) + E_v(t) + I_v(t)$. Mosquitoes enter the susceptible class either through birth (at a constant total birth rate Π_v). They are assumed to die naturally at a per capita rate μ_v or move to the exposed class, and the gametocytes passed on to the midgut of the mosquito after biting an infected human from the exposed, infectious, under treatment or recovered class. The rate of infection of a susceptible mosquito is assumed to be given by the standard incidence force of infection $\Lambda_{hv} = \dfrac{\beta_{hv} b}{N_h}(\zeta_e E_h + \zeta_r R_h + \zeta_t T_h + I_h)$, where β_{hv} is the probability that a bite by a susceptible mosquito on an infected human leads to an infection of the mosquito. Here we introduce the relative infectivities, $0 \le \zeta_e < \zeta_r < \zeta_t < 1$, that account for the reduction in the transmission from, respectively, an exposed, recovered, treated human to susceptible

mosquito. Exposed mosquitoes either die at the rate μ_v or move to the infectious class at rate ν_v and infectious mosquitoes die at the rate μ_v. A pictorial representations of the compartments and flows are shown on Fig. 1.

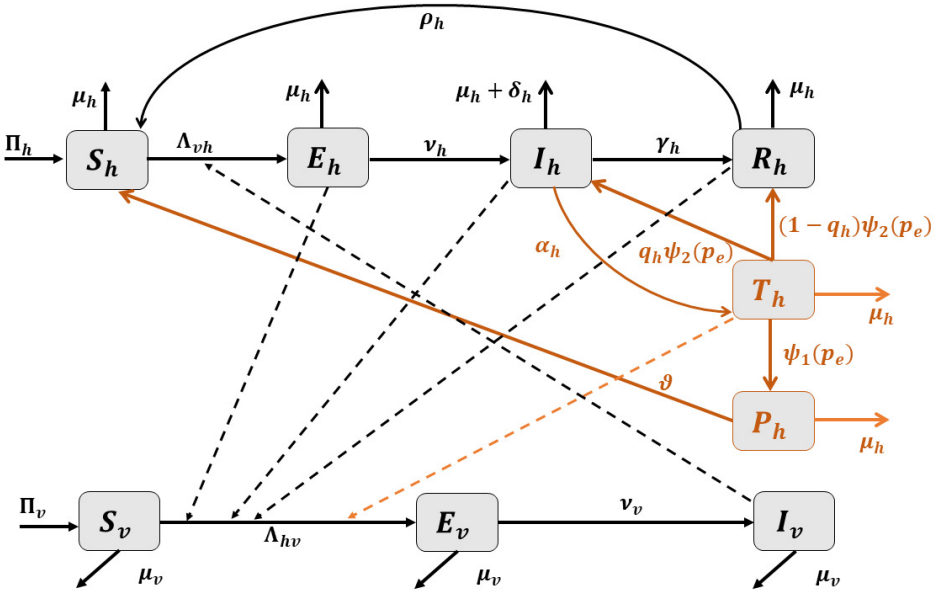

Figure 1: Flow diagram showing the malaria transmission dynamics between human and mosquito populations with a transmission-blocking drug treatment.

Variables	Description	Quasi-dimension
S_h	susceptible humans	H
E_h	exposed humans	H
I_h	infected humans	H
T_h	undergoing treatment humans	H
P_h	protected (successfully treated and noninfective) humans	H
R_h	recovered humans	H
S_v	susceptible mosquitoes	V
E_v	exposed mosquitoes	V
I_v	infectious mosquitoes	V

Table 1: State variables, their description and corresponding quasi-dimension, where the dimension H denotes the number of human-individuals in the population, and the dimension V the number (density) of vectors in the female mosquito population.

2.2 Model Equations

The mathematical model we study in this paper for the transmission dynamics of malaria with TBDs treatment is given by the following non-linear system of ODEs.

$$
\begin{cases}
\dfrac{dS_h}{dt} = \Pi_h + \rho_h R_h + \vartheta P_h - \Lambda_{vh} S_h - \mu_h S_h, \\
\dfrac{dE_h}{dt} = \Lambda_{vh} S_h - (\nu_h + \mu_h)\, E_h, \\
\dfrac{dI_h}{dt} = \nu_h E_h + q_h \psi_2(p_e) T_h - (\delta_h + \gamma_h + \alpha_h + \mu_h)\, I_h, \\
\dfrac{dT_h}{dt} = \alpha_h I_h - \psi_1(p_e) T_h - q_h \psi_2(p_e) T_h - (1 - q_h)\psi_2(p_e) T_h - \mu_h T_h, \\
\dfrac{dP_h}{dt} = \psi_1(p_e) T_h - \vartheta P_h - \mu_h P_h, \\
\dfrac{dR_h}{dt} = \gamma_h I_h + (1 - q_h)\psi_2(p_e) T_h - \rho_h R_h - \mu_h R_h, \\
\dfrac{dS_v}{dt} = \Pi_v - \Lambda_{hv} S_v - \mu_v S_v, \\
\dfrac{dE_v}{dt} = \Lambda_{hv} S_v - (\nu_v + \mu_v)\, E_v, \\
\dfrac{dI_v}{dt} = \nu_v E_v - \mu_v I_v,
\end{cases}
\quad , \tag{1}
$$

where Λ_{vh} and Λ_{hv} are the forces of infections from vector to human and from human to vector, respectively. As mentioned before, they are given by

$$
\Lambda_{vh}(I_v) = \frac{\beta_{vh} b}{N_h} I_v, \qquad \Lambda_{hv}\left(E_h, R_h, T_h, I_h\right) = \frac{\beta_{hv} b}{N_h}\left(\zeta_e E_h + \zeta_r R_h + \zeta_t T_h + I_h\right). \tag{2}
$$

The description of the parameters is given in Table 2.

Adding the rates of change for humans and mosquitoes, respectively, gives

$$
\frac{dN_h}{dt} = \Pi_h - \delta_h I_h - \mu_h N_h \text{ and } \frac{dN_v}{dt} = \Pi_v - \mu_v N_v. \tag{3}
$$

Note that (1) without the fourth and fifth equations, that is, without T_h and P_h variables, is a standard SEIRS-SEI model studied by several authors, see e.g. [16, 19, 46].

3 Mathematical Analysis

In this section we present a mathematical analysis of the model and, in particular, we study its well-posedness, the existence of the equilibria, their stability and the bifurcation behaviour. We observe that since $\psi_1(p_e)$ is the rate at which individuals successfully progress from T_h to P_h, it should be an increasing function of the drug's efficacy p_e. On the other hand, $\psi_2(p_e)$ is the rate at which individuals move back to I_h from T_h due to the failure of the drug and hence it should be a decreasing function of p_e. Thus, in this work we use the simplest functions satisfying these requirements, $\psi_1(p_e) = r_h p_e$ and $\psi_2(p_e) = (1 - p_e)\theta_h$.

3.1 Basic mathematical properties of the model

We begin by ensuring that (1) is well-posed in a biologically feasible domain. Let

$$
\boldsymbol{x}(t) = \Big(S_h(t), E_h(t), I_h(t), T_h(t), P_h(t), R_h(t), S_v(t), E_v(t), I_v(t)\Big) \tag{4}
$$

Parameters	Description	Quasi-dimension
π_h	per capita constant recruitment rate of susceptible humans	T^{-1}
π_v	per capita constant recruitment rate of susceptible mosquitoes	T^{-1}
Π_h	constant total recruitment rate of susceptible humans	HT^{-1}
Π_v	constant total recruitment rate of susceptible vectors	VT^{-1}
β_{vh}	the probability of transmission from infectious vector (mosquito) to susceptible humans during bite	*dimensionless*
β_{hv}	the probability of transmission from infectious humans to susceptible vectors during bite	*dimnsionless*
b	the average biting rate of mosquitoes on humans	$H(VT)^{-1}$
Λ_{vh}	force of infection from infectious vectors to susceptible humans	T^{-1}
Λ_{vh}	force of infection from infectious humans to susceptible vectors	T^{-1}
ν_h	constant progression rate of exposed humans to infected humans	T^{-1}
α_h	constant rate of treatment of infected human with TBD	T^{-1}
ρ_h	waning rate of immunity	
γ_h	natural recovery rate of infected humans by immune response	T^{-1}
p_e	drug efficacy: probability that the drug eventually clears parasites	dimensionless
r_h	rate of individuals treated with TBDs progressing into prophylaxis protection	T^{-1}
ϑ	rate of losing of prophylaxis protection to become susceptibles	T^{-1}
θ_h	rate of slackening/ineffectiveness of TBDs leading to relapse or natural recovery with a probability of q_h or $1-q_h$, resp.	T^{-1}
$\omega_h = q_h\theta_h$	rate of slackening/ineffectiveness of TBDs leading to relapse	T^{-1}
$\sigma_h = (1-q_h)\theta_h$	rate of slackening/ineffectiveness of TBDs leading to a natural recovery	T^{-1}
ζ_e	reduction of the infectivity of exposed humans to vectors	Dimensionless
ζ_r	reduction of the infectivity of recovered humans to vectors	Dimensionless
ζ_t	reduction of the infectivity of under treated humans to vectors	Dimensionless
ν_v	rate at which exposed mosquitoes become infectious	T^{-1}
μ_h	natural death rate of humans	T^{-1}
μ_v	natural death rate of mosquitoes	T^{-1}

Table 2: Parameters, their description and corresponding quasi-dimension.

denote its forward solution when it exists. Let $n \in \mathbb{N}$. For $\boldsymbol{x} = (x_1, \ldots, x_n)$, we use the notation $\boldsymbol{x} \geq 0$ and $\boldsymbol{x} > 0$ if $x_i \geq 0$, respectively, $x_i > 0$ for all $i = 1, \ldots, n$, and hence

$$\begin{aligned} &\mathbb{R}_{\geq 0} = \{x \in \mathbb{R} : x \geq 0\} = [0, \infty),\ \mathbb{R}_{>0} = \{x \in \mathbb{R} : x > 0\} = (0, \infty), \\ &\mathbb{R}^n_{\geq 0} = \{\boldsymbol{x} \in \mathbb{R}^n : \boldsymbol{x} \geq \boldsymbol{0}\},\ \mathbb{R}^n_{>0} = \{\boldsymbol{x} \in \mathbb{R}^n : \boldsymbol{x}\}, \\ &\mathbb{R}^{n*}_{\geq 0} = \{\boldsymbol{x} \in \mathbb{R}^n_{\geq 0} :\ 0 < x_1 + x_2 + \cdots + x_n\}. \end{aligned} \tag{5}$$

Due to biological interpretation, the solutions to (1) are expected to be nonnegative if such are the initial conditions. However, the RHS of (1) is not defined for $N_h = 0$ or $N_v = 0$ and even if we extended the definition by setting it equal to zero in such a case, it would remain discontinuous and thus outside the scope of standard analysis. Thus, though the case of initial conditions satisfying $N_h(0) = N_v(0) = 0$ is obviously tractable as it gives separately evolving disease free human and vector population, we focus

on the interplay of nontrivial human and mosquito populations and thus assume that

$$\Big(S_h(0), E_h(0), I_h(0), T_h(0), P_h(0), R_h(0)\Big) \in \mathbb{R}^{6*}_{\geq 0}, \qquad \Big(S_v(0), E_v(0), I_v(0)\Big) \in \mathbb{R}^{3*}_{\geq 0} \tag{6}$$

Theorem 1 (Solvability, positivity and boundedness of solution) *1. System (1) with initial condition satisfying (6) has a unique global in time solution in $\mathbb{R}^{6*}_{\geq 0} \times \mathbb{R}^{3*}_{\geq 0}$.*

2. The biologically feasible region $\Omega = \Omega_h \times \Omega_v \subseteq \mathbb{R}^{6*}_{\geq 0} \times \mathbb{R}^{3*}_{\geq 0}$, where

$$\Omega_h = \Big\{ (S_h, E_h, I_h, T_h, P_h, R_h) \in \mathbb{R}^{6*}_{\geq 0} : 0 < S_h + E_h + I_h + T_h + P_h + R_h \leq \frac{\Pi_h}{\mu_h} \Big\}, \tag{7}$$

$$\Omega_v = \Big\{ (S_v, E_v, I_v) \in \mathbb{R}^{3*}_{\geq 0} : 0 < S_v + E_v + I_v \leq \frac{\Pi_v}{\mu_v} \Big\} \tag{8}$$

is positively invariant and attracting with respect to system (1).

Proof : System (1) can be written as

$$\boldsymbol{x}' = \boldsymbol{f}(\boldsymbol{x}), \quad \boldsymbol{x}(0) = \boldsymbol{x}_0, \tag{9}$$

where $\boldsymbol{x}$ is defined by (4) with the corresponding initial condition $\boldsymbol{x}_0$ and $\boldsymbol{f}$ is the vector valued function representing the right hand side of the system. Since $\boldsymbol{x}_0 \in \mathbb{R}^{6*}_{\geq 0} \times \mathbb{R}^{3*}_{\geq 0}$, $N_h(0) \neq 0$ and $N_v(0) \neq 0$ and the right hand side of (1) is well defined at $t = 0$. Further, $\boldsymbol{f} \in \mathcal{C}^1(\mathcal{U})$, where $\mathcal{U} = \{\boldsymbol{x} \in \mathbb{R}^9, x_1 + \ldots x_6 > 0 \text{ and } x_7 + x_8 + x_9 > 0\}$ is an open set and thus, for any $\boldsymbol{x}_0 \in \mathcal{U}$, (9) has a unique solution $\boldsymbol{x} : [0, \tau) \to \mathcal{U}$ on some (maximum) interval of existence $[0, \tau)$, where $\tau > 0$ depends on the initial condition.

Next we observe that for all i, $f_i(\boldsymbol{x}) \geq 0$ whenever $\boldsymbol{x} \geq 0$ satisfies $x_i = 0$ and thus the assumptions of [59, Proposition A. 17] are satisfied yielding that any solution $\Big(S_h, E_h, I_h, T_h, P_h, R_h, S_v, E_v, I_v\Big)^T$ of system (1) with initial conditions (6) remains non-negative in the interval of its existence $[0, \tau)$.

Further, adding the first six equations of (1) and using the nonnegativity of I_h and N_h, we get

$$\Pi_h - (\mu_h + \delta_h) N_h \leq \frac{dN_h(t)}{dt} \leq \Pi_h - \mu_h N_h \tag{10}$$

on $[0, \tau)$ and the comparison theorem, [8, 32], yields

$$e^{-(\mu_h+\delta_h)t}\Big(N_h(0) - \frac{\Pi_h}{\mu_h + \delta_h}\Big) + \frac{\Pi_h}{\mu_h + \delta_h} \leq N_h(t) \leq \frac{\Pi_h}{\mu_h} + \Big(N_h(0) - \frac{\Pi_h}{\mu_h}\Big) e^{-\mu_h t}. \tag{11}$$

Similarly, adding the equations for the mosquito population and solving the resulting equation gives

$$N_v(t) = \frac{\Pi_v}{\mu_v} + \Big(N_v(0) - \frac{\Pi_v}{\mu_v}\Big) e^{-\mu_v t} \tag{12}$$

on $[0, \tau)$. Hence, $N_h(t)$ and $N_v(t)$ are bounded from above on $[0, \tau)$. Moreover, using $N_h(0) > 0$ and $N_v(0) > 0$, by continuity, $N_h(t) > 0$ and $N_v(t) > 0$ on $[0, \tau]$. Thus, there are constants $0 < c \leq C$ such that

$$c \leq S_h(t) + E_h(t) + I_h(t) + T_h(t) + P_h(t) + R_h(t) + S_v(t) + E_v(t) + I_v(t) \leq C, \quad t \in [0, \tau),$$

which, together with the nonnegativity of each summand, shows that the solution is in a compact subset of $\mathcal{U}$ for all $t \in [0, \tau)$, Thus, by [52, Corollary 2, Section 2.4], $\tau = \infty$, that is, the solution is global in time.

Finally, by taking the limits as $t \to \infty$ in (11) and (12), we have

$$\lim_{t\to\infty} \sup N_h(t) \leq \frac{\Pi_h}{\mu_h} \quad \text{and} \quad \lim_{t\to\infty} \sup N_v(t) = \frac{\Pi_v}{\mu_v}.$$

In particular, $N_h(t) \leq \max\left\{N_h(0), \frac{\Pi_h}{\mu_h}\right\}$ and $N_v(t) \leq \max\left\{N_v(0), \frac{\Pi_v}{\mu_v}\right\}$ for all $t \geq 0$. This establishes the positive invariance of the set Ω. On the other hand, if $N_h(0) > \frac{\Pi_h}{\mu_h}$, then $N_h(t)$ either decreases below $\frac{\Pi_h}{\mu_h}$ (and thus solution enters Ω in a finite time), or it approaches $\frac{\Pi_h}{\mu_h}$ as $t \to \infty$. Also, $N_v(t)$ converges to $\frac{\Pi_v}{\mu_v}$ as $t \to \infty$. Summarizing, the set Ω is positively invariant and attracts all solutions to system (1) emanating from $\mathbb{R}^{9*}_{\geq 0}$. □

Next, we analyze the malaria model under TBDs treatment, that is, system (1). We begin with determining its disease-free equilibrium (DFE) and the corresponding control reproduction number.

3.2 Disease-free steady equilibrium and control reproduction number

System (1) has a disease free equilibrium point given by

$$\boldsymbol{x}_0^* = \left(\frac{\Pi_h}{\mu_h},\ 0,\ 0,\ 0,\ 0,\ 0, \frac{\Pi_v}{\mu_v},\ 0,\ 0\right).$$

Using the *the next-generation matrix method* based on the approach and notation used in [22, 64], see Appendix 5, we calculate the control reproduction number, $\mathcal{R}_T$ for (1). It is given by

$$\mathcal{R}_T^2 = \mathcal{R}_0^2 \xi\left(\alpha_h\right), \tag{13}$$

where $\mathcal{R}_0$ is the basic reproduction number calculated, when the treatment rate α_h is set to zero in (1) (that is, in the model without TBDs treatment), given by

$$\mathcal{R}_0 = \sqrt{\frac{\Big(\gamma_h\nu_h\zeta_r + \mu_h\nu_h + \nu_h\rho_h + (\Gamma_4\mu_h + \Gamma_4\rho_h)\zeta_e\Big)\Gamma_6 b\beta_{vh}\nu_v}{\Gamma_4(\mu_h+\nu_h)(\mu_h+\rho_h)(\mu_v+\nu_v)\mu_v}} \tag{14}$$

and

$$\xi\left(\alpha_h\right) = \frac{A\alpha_h + 1}{B\alpha_h + 1}$$

with

$$A = \frac{\zeta_e(\mu_h+\rho_h)\Gamma_5 + \nu_h\Big((\mu_h+\rho_h)\zeta_t + \Gamma_2\zeta_r\Big)}{(\Gamma_5+\Gamma_1)\Big((\Gamma_4\zeta_e+\nu_h)(\mu_h+\rho_h) + \nu_h\gamma_h\zeta_r\Big)} \text{ and } B = \frac{\Gamma_5}{\Gamma_4(\Gamma_5+\Gamma_1)}, \tag{15}$$

where

$$\begin{aligned} &\omega_h := q_h\theta_h,\ \sigma_h := (1-q_h)\theta_h,\ \Gamma_1 := (1-p_e)\omega_h,\ \ \Gamma_2 := (1-p_e)\sigma_h,\ \ \Gamma_3 := p_e r_h, \\ &\Gamma_4 := \delta_h + \gamma_h + \mu_h,\ \ \Gamma_5 := \Gamma_2 + \Gamma_3 + \mu_h,\ \ \Gamma_6 = \frac{\Pi_v b\beta_{hv}\mu_h}{\Pi_h\mu_v}. \end{aligned} \tag{16}$$

The condition $\mathcal{R}_T < 1$ is necessary condition to prove the DFE of the system is locally asymptotically stable, [35, 36, 38, 64]. Hence, we have the following theorem.

Theorem 2 (Local stability of DFE) *The disease-free steady state $\boldsymbol{x}_0^*$ of system (1) is locally asymptotically stable if $\mathcal{R}_T < 1$, but unstable if $\mathcal{R}_T > 1$.*

Proof : The proof follows the lines of [64, Theorem 2] and [65, Lemma 2], see, Appendix 5. It can also be proved by determining condition for which all eigenvalues of the model at the DFE have negative real parts, see for e.g. [10, 11, 14, 37].

3.3 Variation of $\mathcal{R}_T$ with respect to α_h

While one could expect $\mathcal{R}_T$ to be a decreasing function of the treatment rate α_h, this is not always the case. In fact, since individuals in the treated class T_h are also infectious, a rapid increase of this class is not always beneficial. Therefore, the effect of the treatment rate α_h on $\mathcal{R}_T$ will depend on other characteristics of the drug, such as p_e, r_h and θ_h etc. This is reflected in the following proposition.

Proposition 1 *Define*

$$\begin{aligned} C_1 :=& \left(\theta_h\left(1-q_h\right)\left(\rho_h+\mu_h-\left(\mu_h+\delta_h\right)\zeta_r\right)-\left(\gamma_h\zeta_r+\mu_h+\rho_h\right)r_h\right)\nu_h, \\ C_2 :=& \nu_h\Big(\left(\mu_h+\gamma_h+\delta_h\right)\left(\mu_h+\rho_h\right)\zeta_t+\left(\mu_h+\delta_h\right)\zeta_r\theta_h\left(1-q_h\right) \\ & -\mu_h\left(\theta_h+\rho_h\right)\left(1-q_h\right)-\mu_h\zeta_r\gamma_h-{\mu_h}^2-\theta_h\rho_h\Big), \\ C_3 :=& \left(\mu_h+\delta_h+\gamma_h\right)\Big(\left(\mu_h+\rho_h+\delta_h+\gamma_h\right)\mu_h\zeta_e+\left(\delta_h+\gamma_h\right)\zeta_e\rho_h \\ & +\left(\mu_h+\rho_h+\gamma_h\zeta_r\right)\nu_h\Big). \end{aligned} \tag{17}$$

R_T is a strictly decreasing function of α_h if and only if $C_1p_e+C_2\leq 0$. In particular,

1. *if $C_1<0$ and $C_2\leq 0$, then $\mathcal{R}_T$ is a decreasing function of α_h for all values of p_e,*
2. *if $C_1<0$ and $C_2\geq 0$, then $\mathcal{R}_T$ is a decreasing function of α_h if and only if $p_e\in[\min\{1,-\frac{C_2}{C_1}\},1]$,*
3. *if $C_1>0$ and $C_2\leq 0$, then $\mathcal{R}_T$ is a decreasing function of α_h for all values of $p_e\in[0,\min\{1,-\frac{C_2}{C_1}\}]$,*
4. *if $C_1>0$ and $C_2\geq 0$, then $\mathcal{R}_T$ is an increasing function of α_h for all values of $p_e\in[0,1]$.*

Proof : By calculating the derivative of $\mathcal{R}_T$ with respect to α_h we obtain that $\mathcal{R}_T$ is a decreasing function of α_h if and only if $A-B\leq 0$, where

$$A-B=\frac{C_1p_e+C_2}{C_3\left(p_er_h+\mu_h+\theta_h(1-p_e)\right)}.$$

Since $0\leq p_e\leq 1$ and $\mu_h>0$, $p_er_h+\mu_h+\theta_h(1-p_e)>0$. Also, clearly $C_3>0$. Hence the sign of $A-B$ is equal to the sign of $C_1p_e+C_2$. Thus, we discuss the following cases:

1. Let $C_1<0$ and $C_2\leq 0$. Then $C_1p_e+C_2\leq 0$ for all values of $p_e\in[0,1]$. Therefore, $\mathcal{R}_T$ is a decreasing function of α_h for all values of $p_e\in[0,1]$.
2. Let $C_1<0$ and $C_2\geq 0$. Then solving $C_1p_e+C_2\leq 0$ for p_e provides $p_e\geq\frac{-C_2}{C_1}\geq 0$. However, p_e is a probability, so $C_1p_e+C_2\leq 0$ is satisfied only if $p_e\in[\min\{1,-\frac{C_2}{C_1}\},1]$.
3. Let $C_1>0$ and $C_2\leq 0$. Then solving $C_1p_e+C_2\leq 0$ for p_e provides $p_e\leq\frac{-C_2}{C_1}$. Since $p_e\in[0,1]$, then $C_1p_e+C_2\leq 0$ if $p_e\in[0,\min\{-\frac{C_2}{C_1},1\}]$.
4. If $C_1>0$ and $C_2\geq 0$, then $C_1p_e+C_2\geq 0$ for $p_e\in[0,1]$ implying that $\mathcal{R}_T$ is increasing with α_h for all values of p_e in $[0,1]$. □

We denote the number $\min\{1,-\frac{C_2}{C_1}\}$ by p_e^c and define it to be the critical efficacy of the TBD. Note that the treatment with TBDs is said to be a perfect treatment if it cures malaria 100% and blocks the formation or maturation of gametocytes, so that the malaria parasites will not be transmitted. So, given $p_e\in[0,1]$, the TBD is a perfect treatment if $p_e=1$ and totally ineffective if $p_e=0$.

In the following remark, we determine the sign of C_1 in terms of the drug's parameters (the same can be done for C_2).

Remark 1 *In Proposition 1, we can observe that*

1. *If* $\rho_h + \mu_h < (\mu_h + \delta_h)\,\zeta_r$, *then* $C_1 < 0$.
2. *If* $\rho_h + \mu_h > (\mu_h + \delta_h)\,\zeta_r$, *and*
   (a) $r_h > \dfrac{\theta_h\,(1-q_h)\,(\rho_h + \mu_h - (\mu_h + \delta_h)\,\zeta_r)}{\gamma_h\zeta_r + \mu_h + \rho_h}$, *then* $C_1 < 0$.
   (b) $r_h < \dfrac{\theta_h\,(1-q_h)\,(\rho_h + \mu_h - (\mu_h + \delta_h)\,\zeta_r)}{\gamma_h\zeta_r + \mu_h + \rho_h}$, *then* $C_1 > 0$.

To investigate graphically how $\mathcal{R}_T$ varies with α_h, we used parameter values collected from previously existing literature, which are summarized in Table 3. Using the parameter values to be the baseline values indicated in Table 3 except that we set $\beta_{vh} = 0.33, \beta_{hv} = 0.833$ and $b = 4.4$, in Subfigure 2a we plotted $\mathcal{R}_T(\alpha_h)$ as the treatment rate α_h increases, while in Subfigure 2b we plotted $\mathcal{R}_T(\alpha_h, p_e)$ when both the treatment rate α_h and efficacy of the TBD, p_e, increase in their non-negative domain. In this case, we get approximately $C_1 = -8.33 \times 10^{-5} < 0$ and $C_2 = -7.42 \times 10^{-5} < 0$ with $\frac{-C_2}{C_1} = -0.859$. Hence, we have the first case in Proposition 1. In Subfigure 2a we fixed $p_e = 0.97$ and let α_h vary from 0 to 1. In this case, the value of $\mathcal{R}_T = \mathcal{R}_T(\alpha_h)$ decreases asymptotically to $\mathcal{R}_0\frac{A}{B}$ as α_h increases and it approaches $\mathcal{R}_0$ when α_h approaches 0; in particular, $\mathcal{R}_T(0) = \mathcal{R}_0$. On Subfigure 2b, $\mathcal{R}_T(\alpha_h, p_e)$ decreases faster since both p_e and α_h are increasing simultaneously.

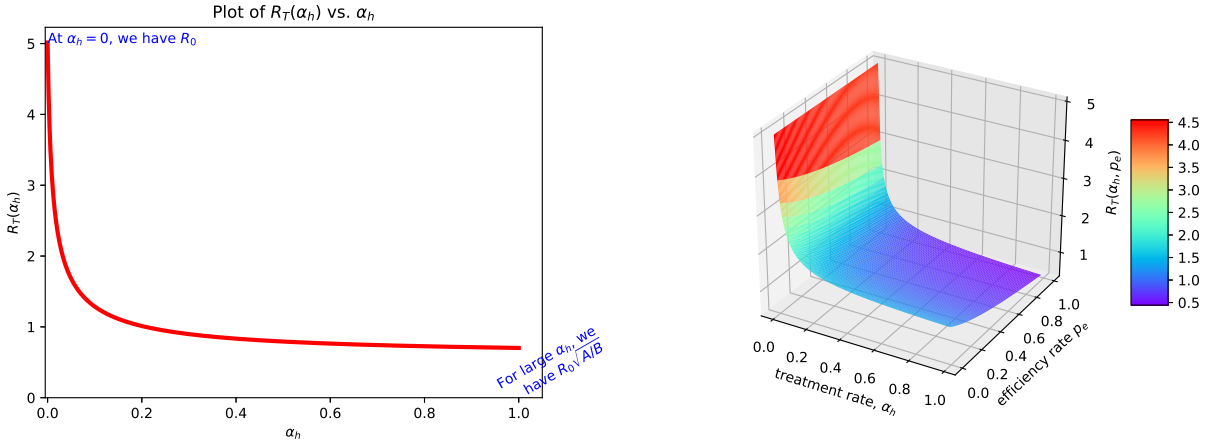

(a) Plot of $\mathcal{R}_T(\alpha_h)$ vs. α_h

(b) Plot of $\mathcal{R}_T(\alpha_h, p_e)$ vs α_h, p_e

Figure 2: A $2-D$ and $3-D$ plots of $\mathcal{R}_T(\alpha_h, p_e)$ given in equation (13) when both the treatment rate, α_h, and efficiency rate of p_e of TBDs increase in their non-negative domain. To plot this figure, we used the baseline values of the parameters indicated in Table 3, except for $\beta_{vh} = 0.33, \beta_{hv} = 0.833$ and $b = 4.4$. These parameter values yield the first case in Proposition 1, that is, $C_1 < 0$ and $C_2 < 0$. In Subfigure 2a, we fixed $p_e = 0.97$ and plotted $\mathcal{R}_T$ as α_h ranges from 0 to 1, and in Subfigure 2b, we let both α_h and p_e to vary. In this case $\mathcal{R}_0\sqrt{\frac{A}{B}} \approx 0.598$ and $\mathcal{R}_0 \approx 5.01$.

We have observed that the control parameters, α_h, p_e, r_h and θ_h play into the variations of $\mathcal{R}_T$. So, in the next subsection, we investigate its normalized sensitivity analysis.

3.4 Sensitivity analysis

In epidemiological modelling, studying the sensitivity of the reproduction number to variations in the model's key parameters is important for choosing the optimal intervention, see [68]. In this section,

Parameter	Range of Possible Values	Baseline Value Used	Dim	Reference
Π_h	$[2.7 \times 10^{-5}, 100]$	5	$H \times day^{-1}$	assumed
Π_v	$[0.002, 200]$	10	$V \times day^{-1}$	assumed
β_{vh}	$[0.01, 1]$	0.022	1	[17]
β_{hv}	$[0.072, 1]$	0.24	1	[17]
b	$[0.1, 30]$	0.33	$H \times V^{-1} \times day^{-1}$	[17]
ν_h	$[0.067, 0.20]$	0.1	day^{-1}	[17]
δ_h	$[1 \times 10^{-5}, 5 \times 10^{-2}]$	1.8×10^{-3}	day^{-1}	[29, 12, 17]
ϑ	$[0.0, 0.1]$	0.05	day^{-1}	[12, 29]
ρ_h	$[5 \times 10^{-4}, 1.1 \times 10^{-2}]$	0.005	day^{-1}	[16]
γ_h	$[3.5 \times 10^{-5}, 0.2]]$	3.5×10^{-3}	day^{-1}	[12, 17]
α_h	$[0, 1]$	0.75	day^{-1}	estimated
p_e	$[0, 1]$	0.97	1	[12, 29]
r_h	$[0, 0.2]$	0.2	day^{-1}	[12]
q_h	$[0, 1]$	0.6	1	assumed
θ_h	$[0.0, 0.2]$	0.15	day^{-1}	estimated
$\sigma_h = (1 - q_h)\theta_h$	$[0.0, 0.2]$	0.06	day^{-1}	[12]
ω_h	$[0.0, 0.2]$	0.09	day^{-1}	estimated
ζ_e	$[0.00001, 1]$	0.001	1	assumed
ζ_r	$[0.005, 1]$	0.05	1	assumed
ζ_t	$[0.02, 1]$	0.08	1	assumed
ν_v	$[0.005, 0.33]$	0.08	day^{-1}	[12, 17]
μ_h	$[2.74 \times 10^{-5}, 0.033]$	4.5×10^{-5}	day^{-1}	[17, 46]
μ_v	$[0.03302, 0.1]$	0.0477	day^{-1}	[17, 46]

Table 3: Parameters, their ranges and baseline values used for this study, dimension and references. Several of the ranges for the parameter values are directly taken from [17], where they used data for the high and low transmission areas. Other parameter ranges are adapted from [12, 29] and some are estimated for the purpose of this study.

we investigate the normalized local sensitivity (or elasticity index) of the control reproduction number $\mathcal{R}_T$ given in (13) to changes of the parameters of the model. Specifically, we are interested in the parameters related to the TBD; that is α_h, p_e, r_h, σ_h, $\omega_h$and ζ_t, where $\sigma_h = (1-q_h)\theta_h$ and $\omega_h = q_h\theta_h$. The normalized local (forward) sensitivity index of the output $\mathcal{R}_T$ to a parameter p, denoted by $\Psi_p^{\mathcal{R}_T}$, is given, [62, 68, 75], by

$$\Psi_p^{\mathcal{R}_T} = \frac{p}{\mathcal{R}_T}\frac{\partial \mathcal{R}_T}{\partial p}.$$

We did not include the analytic expressions of the sensitivity indices since the expression for $\mathcal{R}_T$ involves a square root and its derivatives with respect to the parameters are rather long.

The normalized local sensitivity coefficients given in Table 4 are dimensionless and they show the relative changes of $\mathcal{R}_T$ with respect to a selected parameter p. More specifically, if $\Psi_p^{\mathcal{R}_T} = z$, then a 1% increase in the parameter p results in a z% increase if $z > 0$ (decrease if $z < 0$) in $\mathcal{R}_T$. For example, a 10% increase in the efficacy of the TBD p_e results in a 10.3% reduction in $\mathcal{R}_T$, when other parameters are fixed as in Table 3. So, a highly efficient transmission-blocking antimalarial drug has the potential to reduce transmission of malaria.

Among the parameters appearing in the considered model, $\mathcal{R}_T$ is most sensitive to r_h, the rate at which treated individuals become protected. The next most influential parameter is the efficacy of the transmission-blocking drug p_e and then the treatment coverage rate α_h. $\mathcal{R}_T$ is least sensitive to ω_h, the rate at which the TBD wanes, leading to reinfection.

Para. (p)	short description	Sensitivity Index
p_e	drug efficacy: probability that the drug eventually clears parasites	-1.03
α_h	treatment rate of infected humans with TBDs	-0.363
r_h	rate at which treated individuals with TBDs to successfully progress into prophylaxis protection	-0.135
ζ_t	reduced infectivity of humans under treatment to mosquitoes	$+0.107$
σ_h	rate of slackening/ineffectiveness of TBDs leading recovery due to immunity	$+0.023$
ω_h	rate of slackening/ineffectiveness of TBDs leading to reinfection	$+0.0049$

Table 4: Forward local sensitivity indices of the reproduction number the malaria model with treatment via TBD. We used the baseline values from Table 3 except that we set $\beta_{vh} = 0.33, \beta_{hv} = 0.833$ and $b = 4.4$. These parameter values yield the first case in Proposition 1, that is $C_1 < 0$ and $C_2 < 0$..

3.5 Existence of endemic equilibrium points and bifurcation analysis

In this section we find the equilibria of the model, analyse their stability and, in particular, determine whether the model (1) exhibits a backward bifurcation the existence of which has important implications for the disease control and management.

To determine endemic equilibria, $(S_h^*, E_h^*, I_h^*, T_h^*, P_h^*, R_h^*, S_v^*, E_v^*, I_v^*)$, we solve the algebraic equations by letting the left hand side of system (1) to zero. So, from the first six equations for human compartments we obtain:

$$T_h^* = \frac{\alpha_h}{(\Gamma_5+\Gamma_1)} I_h^*, \quad P_h^* = \frac{\alpha_h \Gamma_3}{(\vartheta+\mu_h)(\Gamma_5+\Gamma_1)} I_h^*, \quad R_h^* = \frac{(\gamma_h(\Gamma_5+\Gamma_1)+\Gamma_2\alpha_h)}{(\rho_h+\mu_h)(\Gamma_5+\Gamma_1)} I_h^*, \tag{18}$$

$$E_h^* = \frac{\Gamma_5(\alpha_h+\Gamma_4)}{\nu_h(\Gamma_5+\Gamma_1)} I_h^*, \quad \Lambda_{vh}^* S_h^* = \frac{\Gamma_5(\nu_h+\mu_h)(\alpha_h+\Gamma_4)}{\nu_h(\Gamma_5+\Gamma_1)} I_h^*, \tag{19}$$

where Λ_{vh}^* is the force of infections of humans at the equilibrium point, given by

$$\Lambda_{vh}^* = \beta_{vh} b \frac{I_v^*}{N_h^*}. \tag{20}$$

Observe that $\Lambda_{vh}^* = 0$ if and only if $I_v^* = 0$. From the second equation of (19), either $\Lambda_{vh}^* = 0$ which implies that $I_h^* = 0$, and hence we obtain the DFE, or $\Lambda_{vh}^* \neq 0$, implying $I_h^* \neq 0$. Moreover, from the second equation of (19) and using the expression of Λ_{vh}^* in (20), we obtain $\beta_{vh} b \frac{I_v^*}{N_h^*} S_h^* = \frac{\Gamma_5(\nu_h+\mu_h)(\alpha_h+\Gamma_4)}{\nu_h(\Gamma_5+\Gamma_1)} I_h^*$. Thus $I_v^* \neq 0$ yields $S_h^* = \frac{\Gamma_5(\nu_h+\mu_h)(\alpha_h+\Gamma_4)N_h^*}{\nu_h(\Gamma_5+\Gamma_1)\beta_{vh} b I_v^*}$. From (3) we see that the equilibria for the total populations are

$$N_h^* = \frac{\Pi_h - \delta_h I_h^*}{\mu_h} \text{ and } N_v^* = \frac{\Pi_v}{\mu_v}.$$

Hence, an endemic equilibrium point exists if I_h lies between $0 < I_h^* < \frac{\Pi_h}{\delta_h}$.

Next, from the three equations for the mosquito population in (1) at equilibrium we obtain

$$S_v^* = \frac{\Pi_v}{\Lambda_{hv}^* + \mu_v}, \quad E_v^* = \frac{\Lambda_{hv}^*}{\nu_v+\mu_v} S_v^*, \quad I_v^* = \frac{\nu_v}{\mu_v} E_v^* = \frac{\nu_v}{\mu_v(\nu_v+\mu_v)} \Lambda_{hv}^* S_v^*. \tag{21a}$$

Hence, we have

$$I_v^* = \frac{\nu_v \Pi_v}{\mu_v(\nu_v+\mu_v)} \frac{\Lambda_{hv}^*}{\Lambda_{hv}^* + \mu_v}, \tag{21b}$$

where Λ^*_{hv} is the force of infections of mosquitoes at the equilibrium point, given by

$$\Lambda^*_{hv} = \beta_{hv} b \frac{\zeta_e E^*_h + \zeta_t T^*_h + \zeta_r R^*_h + I^*_h}{N^*_h} = C_0 \frac{I^*_h}{N^*_h}, \tag{22}$$

so that $I^*_v = K_0 C_0 \dfrac{I^*_h}{C_0 I^*_h + \mu_v N^*_h}$, where K_0 and C_0 are given in Appendix. Now, substituting (21b) into (20), we get

$$\Lambda^*_{vh}\Lambda^*_{hv}\mu_v(\nu_v + \mu_v)N^*_h + \Lambda^*_{vh}\nu_v^2(\nu_v + \mu_v)N^*_h - \beta_{vh} b \nu_v \Pi_v \Lambda^*_{hv} = 0 \tag{23}$$

and, after long computations, we get $\Lambda^*_{hv} = \dfrac{C_{hv}\phi_8\Lambda^*_{vh}}{\phi_1 + \phi_7\Lambda^*_{vh}}$. Hence, (23) becomes

$$a_0\Lambda^{*2}_{vh} + a_1\Lambda^*_{vh} + a_2 = 0, \tag{24}$$

where

$$a_0 = \mu_v K_7 \phi_7 (C_{hv}\phi_8 + \mu_v\phi_7), \tag{25}$$

$$\begin{aligned} a_1 &= C_{hv}\phi_8\mu_v K_7\phi_1 + 2\phi_1\phi_2\mu_v^2 K_7 + C_{vh}\nu_v\Pi_v C_{hv}\phi_8(D_{01} - D_{00}) \\ &= \frac{\mu_v^2 K_7\phi_1^2}{\mu_h}\Big(\frac{C_{hv}\phi_8\mu_v K_7\phi_1 + 2\phi_1\phi_2\mu_v^2 K_7 + C_{vh}\nu_v\Pi_v C_{hv}\phi_8 D_{01}}{\mu_v^2 K_7\phi_1^2} - \mathcal{R}_T^2\Big), \end{aligned} \tag{26}$$

$$a_2 = \mu_v^2 K_7\phi_1^2 - C_{vh}\nu_v\Pi_v C_{hv}\phi_8 D_{02} = \mu_v^2 K_7\phi_1^2\Big(1 - \mathcal{R}_T^2\Big), \tag{27}$$

where $K_1, \cdots, K_7$, $\phi_1, \cdots, \phi_8$ and D_{00}, D_{01} D_{02} are positive quantities given in Appendix. Here, the expression for $\mathcal{R}_T^2$ from (13) can be written as $\mathcal{R}_T^2 = \dfrac{C_{vh}\nu_v\Pi_v C_{hv}\phi_8 D_{02}}{\mu_v^2 K_7\phi_1^2}$.

By using the properties of roots of a quadratic equation in (24), we summarize the existence and the number of EE point(s) scenarios. We use the approach introduced in [50]. For this, we rewrite (24), as

$$\Lambda^{*2}_{vh} + b(K - \mathcal{R}_T^2)\Lambda^*_{vh} + c(1 - \mathcal{R}_T^2) = 0, \tag{28}$$

where

$$b = \frac{\mu_v^2 K_7\phi_1^2}{\mu_h\mu_v K_7\phi_7(C_{hv}\phi_8 + \mu_v\phi_7)}, \quad c = \frac{\mu_v^2 K_7\phi_1^2}{\mu_v K_7\phi_7(C_{hv}\phi_8 + \mu_v\phi_7)},$$
$$K = \frac{C_{hv}\phi_8\mu_v K_7\phi_1 + 2\phi_1\phi_2\mu_v^2 K_7 + C_{vh}\nu_v\Pi_v C_{hv}\phi_8 D_{01}}{\mu_v^2 K_7\phi_1^2}.$$

Clearly, $b > 0$, $C > 0$ and $K > 0$. Solving this quadratic equation for Λ_{vh} yields

$$\Lambda_{vh} = \frac{-b(K - \mathcal{R}_T^2) \pm \sqrt{b^2(K - \mathcal{R}_T^2)^2 - 4c(1 - \mathcal{R}_T^2)}}{2},$$

provided that this exists as a non-negative real number. We note that the equilibrium points in (**??**) are written in terms of I^*_h, and thus, to obtain the endemic equilibria once we solve (24) for Λ^*_{vh}, we can obtain I^*_h.

Now to investigate for non negative roots of (24), let us denote its discriminant by

$$\Delta(\mathcal{R}_T^2) := b^2(K - \mathcal{R}_T^2)^2 - 4c(1 - \mathcal{R}_T^2) = b^2\mathcal{R}_T^4 + (4c - 2kb^2)\mathcal{R}_T^2 + b^2k^2 - 4c.$$

We require that $\Delta(\mathcal{R}_T^2) \geq 0$, otherwise the quadratic equation (28) does not have real roots, and hence there is no endemic equilibrium for such values of $\mathcal{R}_T^2$.

Hence, solving $\Delta(\mathcal{R}_T^2) = 0$ yields

$$\mathcal{R}_{T_1} = \frac{\sqrt{Kb^2 - 2c - 2\sqrt{b^2c(1-K)+c^2}}}{\sqrt{2}b}, \quad \mathcal{R}_{T_2} = \frac{\sqrt{Kb^2 - 2c + 2\sqrt{b^2c(1-K)+c^2}}}{\sqrt{2}b}, \tag{29}$$

provided that they exist as real roots. Recalling that $0 \leq \mathcal{R}_T^2 < 1$ if and only if $0 \leq \mathcal{R}_T < 1$, we have the following theorem.

Theorem 3 *(1) If $\mathcal{R}_T > 1$, then equation (28) has one positive root and thus model (1) has one EE and a DFE (which always exists).*

(2) If $K \geq 1$, then equation (28) exhibits a forward bifurcation, that is, it has

(i) no positive roots if $0 \leq \mathcal{R}_T \leq 1$, in which case, (1) has only a DFE,

(ii) a unique positive root if $\mathcal{R}_T > 1$, in which case, (1) has one EE and a DFE.

(3) If $0 < K < 1$, then $0 < \mathcal{R}_{T_2} < 1$ and equation (28) exhibits backward bifurcation, that is, (28) has

(i) no positive roots if $0 \leq \mathcal{R}_T < \mathcal{R}_{T_2}$, and (1) has only a DFE,

(ii) one double positive root if $\mathcal{R}_T = \mathcal{R}_{T_2}$, and (1) has one EE and a DFE,

(iii) two positive real roots if $\mathcal{R}_{T_2} < \mathcal{R}_T < 1$, and (1) has two EEs and a DFE,

(iv) a unique positive root if $\mathcal{R}_T \geq 1$ so that, (1) has one EE and a DFE.

Proof : The proof follows similar steps to the proof of [50, page 3] for the case $b > 0$, $c > 0$ and $K > 0$. We note here that the existence of positive endemic equilibrium point(s), when $\mathcal{R}_T < 1$ for our model

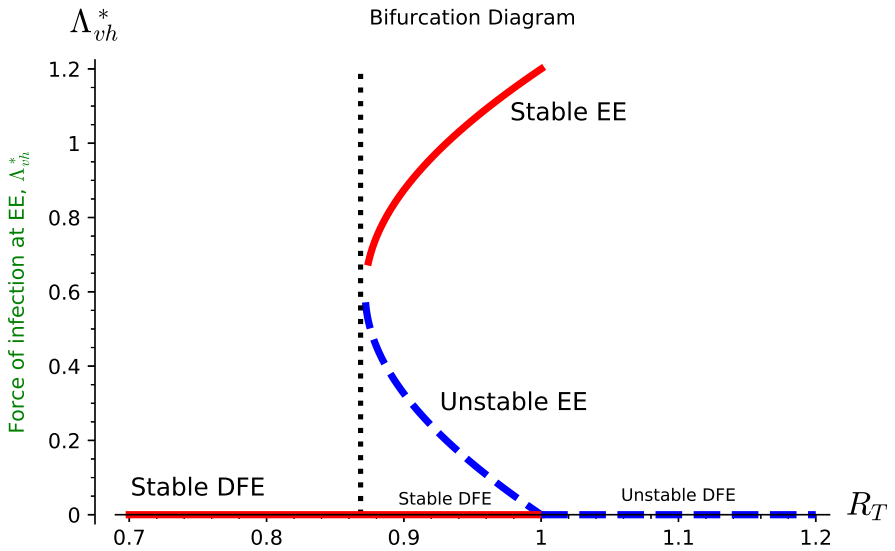

Figure 3: Backward bifurcation diagram showing the cases considered in Theorem 3. We used the baseline parameter values in Table 3 and we set $p_e = 0.75$, $\zeta_e = 0.01$, $\zeta_r = 0.05$, $\zeta_t = 0.08$, $b = b = 2.0$, and we obtained $\mathcal{R}_T = 0.971$ and $\mathcal{R}_{T_2} \approx 0.8689$ so that $\mathcal{R}_{T_2} < \mathcal{R}_T < 1$, which shows the existence of backward bifurcation [30, 53].

can be also shown using the method applied in [34].

The main reason to investigate the occurrence of backward bifurcations is that if it occurs in a model, then the usual condition $\mathcal{R}_T < 1$ is not sufficient to completely control the transmission of the disease and $\mathcal{R}_T$ should be reduced further, below another threshold, to ensure the eradication of the disease. Thus, understanding the reasons a backward bifurcation and finding possible ways of preventing it is of utmost importance, [30, 34, 53].

Remark 2 *From the bifurcation theorem (Theorem 3), we see that a TBD is capable of eliminating malaria infection from the population if and only if* $\mathcal{R}_T < \mathcal{R}^{\#}$, *where*

$$\mathcal{R}^{\#} = \begin{cases} 1 \text{ if } K > 1 \text{ (forward bifurcation)} \\ \mathcal{R}_{T_2} \text{ if } K < 1 \text{ (backward bifurcation)} \end{cases}.$$

On the other hand, we have $\mathcal{R}_T < \mathcal{R}^{\#}$ if and only if $\frac{\mathcal{R}_0^2(A\alpha_h+1)}{B\alpha_h+1} < \mathcal{R}^{\#2}$, that is,

$$(\mathcal{R}_0^2 A - B\mathcal{R}^{\#2})\alpha_h < (\mathcal{R}^{\#2} - \mathcal{R}_0^2),$$

where A and B are defined in (15). Hence, we discuss the following cases.

1. If $\mathcal{R}_0^2 A - B\mathcal{R}^{\#2} > 0$, then $\mathcal{R}_T < \mathcal{R}^{\#}$ if and only if $\alpha_h < \dfrac{\mathcal{R}^{\#2} - \mathcal{R}_0^2}{\mathcal{R}_0^2 A - B\mathcal{R}^{\#2}}$.
2. If $\mathcal{R}_0^2 A - B\mathcal{R}^{\#2} < 0$, then $\mathcal{R}_T < \mathcal{R}^{\#}$ if and only if $\alpha_h > \dfrac{\mathcal{R}^{\#2} - \mathcal{R}_0^2}{\mathcal{R}_0^2 A - B\mathcal{R}^{\#2}}$. Note that the sign of $\mathcal{R}^{\#} - \mathcal{R}_0$ plays a role here.

Remark 3 *We have shown numerically that both the above conditions can happen (at least mathematically). However, for epidemiological interpretations (for realistic parameter values of our model), we consider only the condition* $\mathcal{R}_0^2 A - B\mathcal{R}^{\#2} < 0$. *In such a case,* $\mathcal{R}_T < \mathcal{R}^{\#}$ *if and only if*

$$\alpha_h > \alpha_h^{\#} := \frac{\mathcal{R}^{\#2} - \mathcal{R}_0^2}{\mathcal{R}_0^2 A - B\mathcal{R}^{\#2}} = \begin{cases} \dfrac{1 - \mathcal{R}_0^2}{\mathcal{R}_0^2 A - B} \text{ if } K > 1 \text{ (forward bifurcation)} \\ \dfrac{\mathcal{R}_{T_2} - \mathcal{R}_0^2}{\mathcal{R}_0^2 A - B\mathcal{R}_{T_2}} \text{ if } K < 1 \text{ (backward bifurcation)} \end{cases},$$

where A *and* B *are given in Equations* (15), *and* $\mathcal{R}_{T_2}$ *is given in Equation* (29).

This equation implies that in clinical trials, for any efficacious transmission-blocking antimalarial drug to effectively control malaria transmission, we require $\alpha_h > \alpha_h^{\#}$. We note that K is also a function of α_h. So the formula above should be understood as follows. For a given α_h we determine K and on this basis we vary other parameters to make $\alpha_h^{\#}$ smaller than α_h.

We see that $\alpha_h^{\#}$ is the critical treatment coverage rate, which is the minimum coverage rate value above which the TBD is capable of eradicating malaria infection from the human population and is able to block transmission of malaria parasites, assuming that the drug is efficacious. Note that $\alpha_h^{\#}$ is obtained when $\mathcal{R}_T = \mathcal{R}^{\#}$.

Particularly, when $K > 1$, (no backward bifurcation), that is, when $\mathcal{R}^{\#} = 1$, the disease will be eliminated if and only if

$$\alpha_h > \alpha_h^c = \frac{1 - \mathcal{R}_0^2}{\mathcal{R}_0^2 A - B}.$$

Next we will investigate how $\alpha_h^{\#}$ changes with respect to p_e when $K > 1$, using the parameter values in Table 3. Figure 4 shows the graph of the critical value $\alpha_h^{\#} = \alpha_h^c(p_e) = \dfrac{1 - \mathcal{R}_0^2}{\mathcal{R}_0^2 A(p_e) - B(p_e)}$ as p_e ranges between 0 and 1. We can see from Figure 4 that when $p_e = 95\%$, the minimum treatment coverage rate α_h^c is approximately 39%. However, when p_e is 55%, we observe that the minimum coverage rate jumps to 43%.

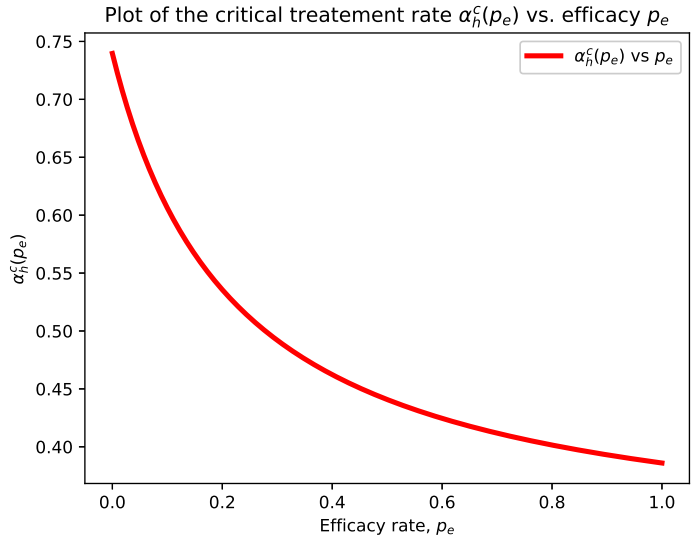

Figure 4: A plot of $\alpha_h^c(p_e)$ as a function of the efficiency rate p_e. To plot this figure, we used the parameter values to be the baseline values indicated in Table 3 except that we changed $b = 4.48 = b$ and $\mu_h = 4.5 \times 10^{-4}$. For these set of parameter values, $A_0 - B_0 < 1$.

Remark 4 *We note that the mathematical analysis is presented here just to illustrate basic local properties of the model. The main aim of the paper is to introduce a model providing a mathematical framework for studying population effects of transmission-blocking drugs and providing support for current biochemical research, [1, 9, 15, 21, 61, 57, 66]. Since mathematically the model is similar to other epidemiological models such as discussed [2, 10, 11, 14, 13, 19, 37, 40, 65], further stability results concerning the disease free equilibrium can be studied using methods developed in [35] or [10, 14]. Nevertheless, as we already showed the existence of an endemic equilibrium when $\mathcal{R}_T < 1$, the DFE cannot by globally asymptotically stable in this case. Similarly, the stability of endemic equilibrium which occurs when $\mathcal{R}_T > 1$ can be studied using the methods of [10, 11, 37]. However, due to the large size of the model, the resulting conditions would be cumbersome and not that informative.*

4 Data fitting and parameter values estimation

In order to calibrate mathematical models, researchers require time series data that describe changes in one or more states of the studied system and use them to fit the model to observations so that its solutions can be used to predict the behaviour of the real system in situations for which experimental data are not available. Model fitting involves parameter estimation, that is, identification of the parameter values that best account for an existing set of data, and then fit the solution curves of the state variables in the model. It also provides statistical tests for parameters [23]. In this section, we present curve fitting and provide parameters estimations by fitting data into the model given in (1).

4.1 Data description

The World Health Organization (WHO)-Global Health Observatory (GHO) and the Institute of Health Metrics and Evaluation (IHME)-Global Burden of Disease (GBD), estimate the number of malaria deaths and cases every year and the corresponding sets of data can be obtained from the WHO-GHO, [72], and the IHME-GBD, [33], web-sites. These estimated data for number of deaths and cases are are done per country and malaria regions. As we mentioned in Introduction, some of the commonly used antimalarial drugs block malaria transmission with certain efficacy. Thus, we fit the full model (1)

with a TBD treatment, using the data from IHME-GBD for the estimated number of malaria caused deaths in the years $1998-2017$ for Sub-Saharan Africa as a region (these data are also summarized in the website of "our world in data" [54]). Hence, we used initial data to be the population sizes of Sub-Saharan Africa in $t_0 = 1998$. That is, $S_h(t_0) = 6 \times 10^8$, [63, 73], $E_h(t_0) = 3.7 \times 10^8$ assumed, $I_h(t_0) = 2.2 \times 10^6$, [33, 54], $\delta_h I_h(t_0) = 696652$, [33, 54], $T_h(t_0) = P_h(t_0) = 0$, $S_v(t_0) = 5 \times 10^6$, and $E_v(t_0) = 2 \times 10^5$, $I_v(t_0) = 1 \times 10^5$, all assumed. We assume the transmission-blocking efficacy p_e of standard drugs in this period was 0.55 and the introduction of modern TBDs is accounted for by increasing p_e after 2017.

4.2 Curve fitting and parameter values estimation

In order to fit and estimate the parameters of system (1), we used the "lmfit" which is a non-linear least-squares minimization and curve-fitting package in Python programming language. As it is directly mentioned in [45], initially inspired by (and named after) the Levenberg-Marquardt method, "lmfit" provides a high-level interface to non-linear optimization and curve fitting problems for Python. It builds on and extends many of the optimization methods of *scipy.optimize*. We preferred to use "lmfit" since it provides a number of useful enhancements to data fitting problems such as the ease of changing fitting algorithms without changing the objective function, improved estimation of confidence intervals, improved curve-fitting and many pre-built models for common line shapes, [45]. We note here that for many data fitting processes, in order to do a non-linear least-squares fit of a model to data, the main task is to write an objective function that takes the values of the fitting variables and calculates an array of values that are to be minimized, typically in the least-squares sense, and the objective function should return an array of (data-model), perhaps scaled by some weighting factor, ϵ, such as the inverse of the uncertainty in the data. For such a problem, unlike to a traditional non-linear fit, the chi-square χ^2 statistic is often defined as [45]:

$$\chi^2 = \sum_{i=0}^{n-1} \frac{\left[y_{t_i}^{meas} - y_{t_i}^{model}\right]^2}{\epsilon_i^2},$$

where $y_{t_i}^{meas}$ is the set of measured data at time point t_i, $y_{t_i}^{model}$ is the solution of the model at time t_i. Most often $\epsilon_i = 1$ for all $i = 1, 2. \cdots, n-1$.

We first write (1) as

$$\dot{\boldsymbol{y}} = \boldsymbol{f}\left(t, \boldsymbol{y}, \boldsymbol{\theta}\right), \qquad \boldsymbol{y}(t_0) = \boldsymbol{y}_0, \tag{30}$$

where, $\boldsymbol{y} = (y_0, \cdots, y_8)$ represents the vector of the model variables , $\boldsymbol{f} = (f_0, f_2, \cdots, f_8)^T$ is vector of right side functions and $\boldsymbol{\theta}$ is vector of unknown of parameters of the model. The main procedure is to estimate model parameters by searching for the vector of parameters $\tilde{\boldsymbol{\theta}} = \left(\tilde{\theta_1}, \tilde{\theta_2}, \cdots, \tilde{\theta_m}\right)$, where m is the number of model parameters, that minimizes the sum of squared differences between the observed (measured) data and the corresponding model solution [18], given as

$$\tilde{\boldsymbol{\theta}} = \arg\min \sum_{i=0}^{n-1} \left(y_{t_i}^{meas} - y_{t_i}^{model}\right)^2,$$

subject to system (30). To get the best fit we use the temporal variation of the residuals given by

$$res(t_i) = f(t_i, y_{t_i}^{meas}, \boldsymbol{\theta}) - y_{t_i}^{meas}.$$

For the purpose of data analysis, we used inferential qualitative data analysis methods which show correlations, regression and analysis of covariance to generalize results and predictions. Our algorithm provided the "Fit Statistics" such as chi-square, reduced chi-square, bayesian info criteria, akaike info criteria and correlations. However, we did not present the values as they are not important to our objective here. A fitted curve is shown on Figure 5. Using the algorithm used to obtain the fitted curve, we estimates values for the model parameters. Depending on the method of estimation they use,

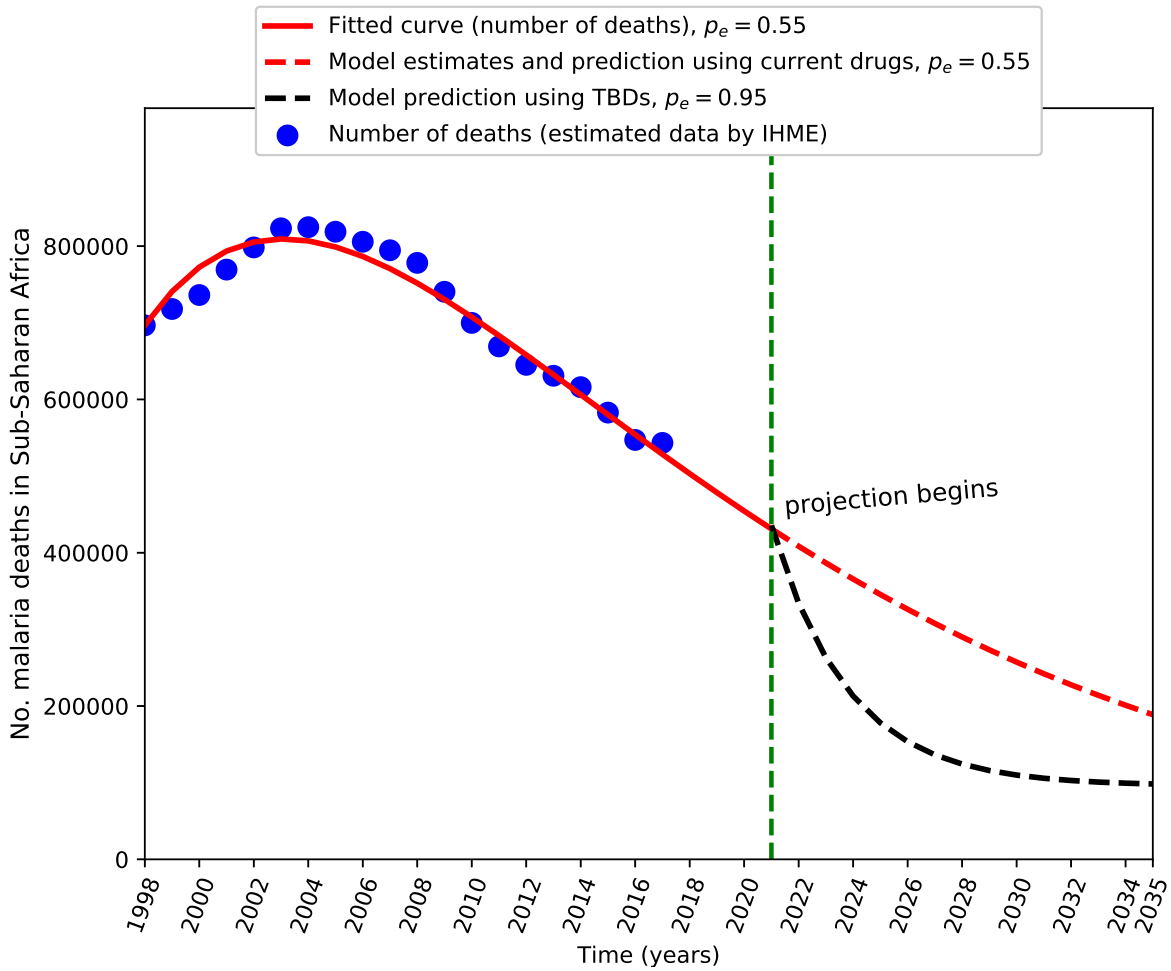

Figure 5: A fitted curve for malaria caused deaths, δI_h, for the model under treatment via TBDs, (system (1)), using data from IHME-GBD [27, 54] in years $1998 - 2017$ for Sub-Saharan Africa as one region. While fitting the curve, we also conducted parameter values estimation using our fitting algorithm and we got, measured per year, $\rho_h = 1.42571563$, $C_v = 0.07183827$, $C_h = 2.60330271$, $\mu_h = 1.1457 \times 10^{-5}$, $\nu_h = 0.21382367$, $\delta_h = 0.000695$, $\gamma_h = 9.7967 \times 10^{-7}$, $\Pi_h = 3.9714 \times 10^6$, $\Pi_v = 4.0012 \times 10^6$, $\nu_v = 0.08502137$, $\mu_v = 8.87970645$, $\zeta_e = 0.99918687$, $\zeta_r = 0.03958800$, $\zeta_t = 0.00336839, \vartheta = 0.23576108$, $\omega_h = 1.37089493$, $r_h = 1.4245 \times 10^{-6}$, $\sigma_h = 0.0035$, $p_e = 0.38365352$ and $\alpha_h = 0.28695193$. Note that here the time unit is one year, in contrast to in Table 3 where the unit of time is one day.

there are differences in the data obtained from WHO and IHME. There is also a difference between the number of estimated and reported confirmed cases or deaths in the WHO data system. We remark that we did not use data from WHO since their data are limited to the years $2010 - 2017$ and our model has more parameters as compared to the number of data points in these years.

Remark 5 *We observe that the fitted demographic parameters are not realistic which is due to the simplified logistic model used to describe the demographic processes, see [43, Pages 36-37]. Our interest is, however, in analyzing the effect of the TBD on the evolution of the disease and thus we continue with the current model in a slightly artificial demographic scenario, for the sake of mathematical tractability of the problem. In reality, in Sub-Saharan Africa regions, the average life-expectancy at birth of humans as of* 2018 *is* 61.25 *years, [60], and thus approximately* $\mu_h = 0.016$ *per year, with a rough estimate of* $\Pi_h = 30 \times 10^6$ *total births per year on average, [63, 73].*

Our model results fit well to the data and it reflects the transmission dynamics of malaria in Sub-Saharan Africa as stated by the IHME-GHO and WHO. Estimated and reported numbers by both WHO and IHME have shown that the number of malaria caused deaths in Sub-Saharan Africa has

fallen since 2007. The fitted solid red curve is obtained by assuming that the transmission-blocking efficacy of common drugs was 0.55. Here we see that the rate at which successfully treated infectious humans become prophylaxis protected, r_h, is very small, with estimated value of $r_h = 1.43 \times 10^{-6}$, see Fig. 5.

To predict the number of malaria deaths in Sub-Saharan Africa, we projected the fitted model by extending the time period up to the year 2035 with the same 55% blocking efficacy of the drugs (the red dashed curve on Figure 5). Thus, using our model with a 55% transmission-blocking, there will be approximately 349185 number of malaria caused deaths and 132.6 million number of cases in Sub-Saharan Africa in the year 2025. These number will be reduced approximately to 214170 deaths and 79.6 million cases in 2035.

This is compared with a scenario in which a 95% efficacious TBD becomes available from 2021, see the dashed black curve. The model predicts that in Sub-Saharan Africa there will be an estimated 178043 malaria related deaths in 2025 and 98343 related deaths in 2035. Since, according to IHME-GBD, [27, 54], there were approximately 543289 malaria deaths in the region in 2017. Thus our model projects at least an 81.8% reduction in the number of malaria deaths by 2035 and, comparing drugs with 55% and 95% efficacy, using the later will save 115827 lives in 2035 alone. This translates into the cumulative number 2.1 million lives saved between 2020 and 2035 if we manage to improve the efficacy of transmission-blocking from 55% to 95%.

It is important to note that this effect is obtained just by using a 95% efficacious TBD starting from 2021 and holding all other malaria control measures (that is, parameters of the model) unchanged. If, in addition, other control measures, such the treatment coverage, are applied the number of malaria cases and deaths will be reduced even more.

To observe how varying the treatment coverage rate and the efficacy impacts the dynamics of malaria model (1), we simulate the system for different values of α_h and p_e, as can be seen on Figures 6 and 7. For both figures we used parameter values obtained from our data fitting, which are listed in the caption of Figure 5, except for Figure 6, where we let the treatment coverage rate to have values $\alpha_h = 0,\ 0.001,\ 0.08,\ 0.2,\ 0.5,\ 0.75,\ 0.90$, with $p_e = 0.39$ fixed, whereas in Figure 7, we fixed $\alpha_h = 0.29$ and let p_e to take efficiency rates of $0\%,\ 25\%,\ 60\%,\ 75\%,\ 97\%$ and 100%.

The trajectories on Figure 6 show that when $\alpha_h = 0$, that is, there are no individuals undergoing the treatment, the trajectories for individuals under treatment or who are prophylaxis protected remain zero. When α_h begins to increase, then the trajectories of T_h and P_h continue to rise. When $\alpha_h < 0.2$, the disease can not be eliminated completely in short period of time (at least it requires more than 100 years), see Subfigures 6a and 6b for $\alpha_h = 0$, $\alpha_h = 0.01$, $\alpha_h = 0.08$ and $\alpha_h = 0.2$.. However, when the treatment coverage rate is increased to $\alpha_h = 0.5$, the number of infected individuals and malaria deaths decreases radically, see Subfigures 6a and 6b for $\alpha_h = 0.5$, $\alpha_h = 0.75$ and $\alpha_h = 0.9$. In Subfigures 7a and 7b, we simulated the numbers of infected humans and malaria caused deaths as we vary the efficacy rate p_e of the transmission-blocking drug. The results in these subfigures show that the number of infected individuals is highly sensitive to the p_e and a 97% efficacious TBD can result in a 100% control of transmission of malaria in a long run. From Subfigure 7c, we observe that treating a malaria patient with a zero efficacy TBD does not have any impact on the patient and thus the trajectory for $p_e = 0$ stays constant for larger times. However, when the TBD is more than 25% efficacious, then individuals will get treated and move to class P_h. In Subfigure 7d, it is shown that when $p_e = 0$, the solution trajectory for P_h remains zero since no one has got successfully treated. Solution trajectories for the total human population with 55% efficacious TBD and the treatment coverage rate of $\alpha_h = 0.35$ are shown on Subfigure 7e. We recall that we use the initial data introduced in Section 4.1.

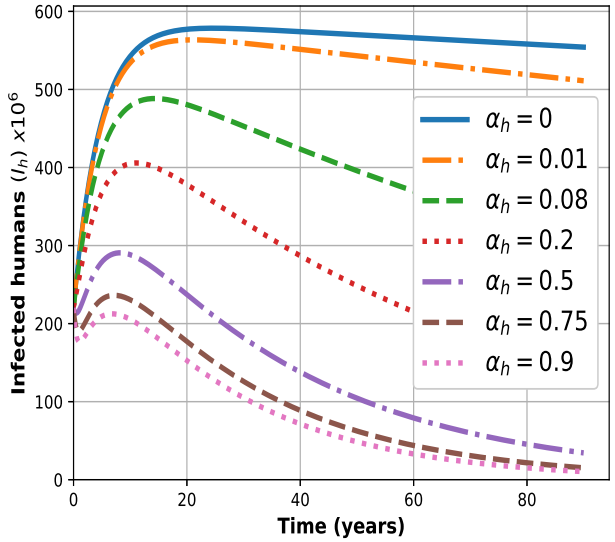

(a) Effect of varying α_h on I_h

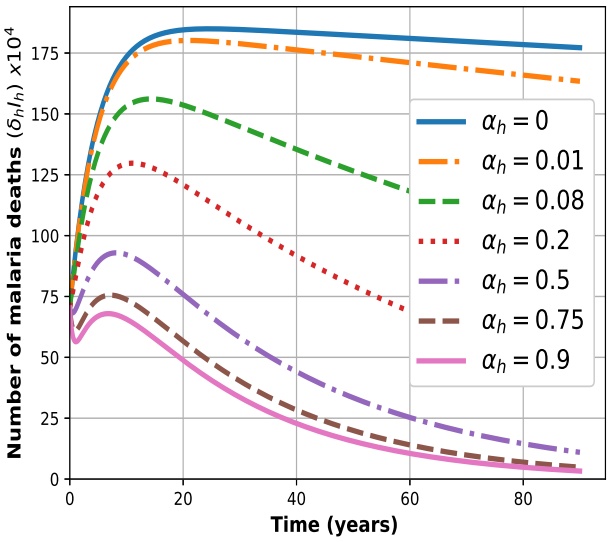

(b) Effect of varying α_h on $\delta_h I_h$

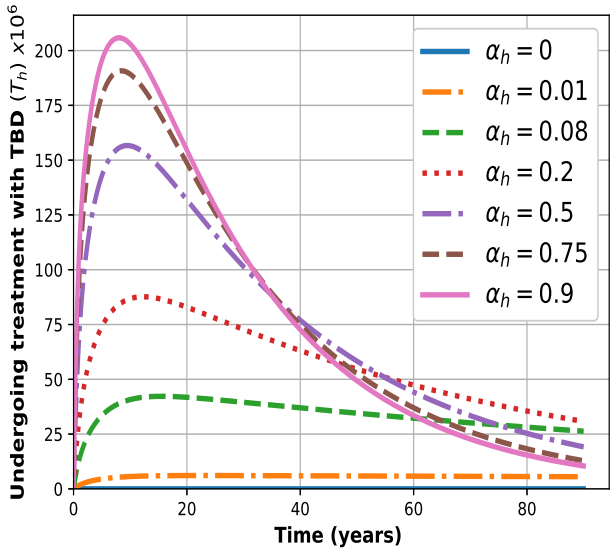

(c) Effect of varying α_h on T_h

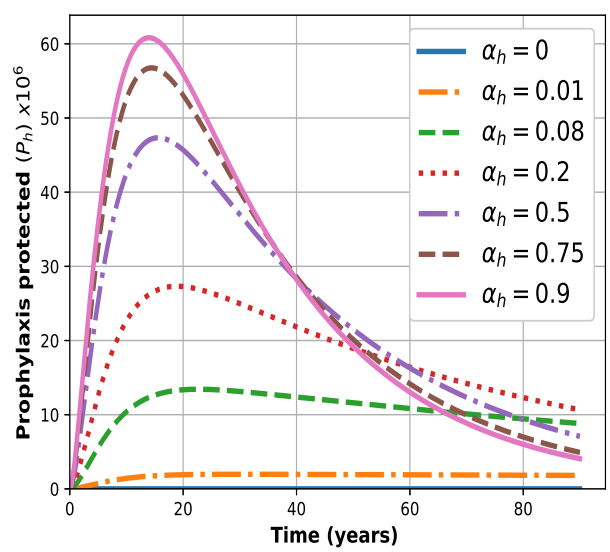

(d) Effect of varying α_h on P_h

Figure 6: Simulations showing the effect of varying the parameter α_h on the number of and proportion of infected, undergoing treatment with TBDs and prophylaxis protected humans. We used parameter values to be the estimated values obtained from data fittinf and are listed on the caption of Figure 5. Here, we let α_h to vary between 0 and 1. We used the following initial data; $S_h(t_0) = 800\times10^6$, $E_h(t_0) = 369.3 \times 10^6$, $I_h(t_0) = 220 \times 10^6$, $T_h(t_0) = 0 = P_h(t_0) = R_h(t_0)$, $S_v(t_0) = 5 \times 10^6$, $E_v(t_0) = 200000$, and $I_v(t_0) = 100000$, where $t_0 = 0$ corresponds to the year 1998. These initial data have been used as initial guess for the purpose of data fitting on Figure 5.

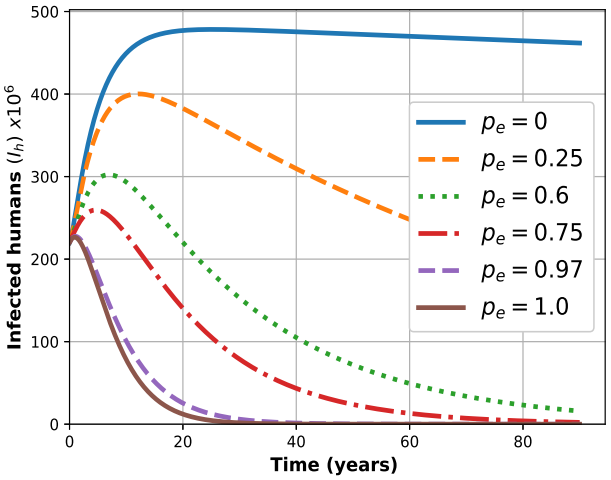

(a) Effect of varying p_e on number of in infected humans, I_h

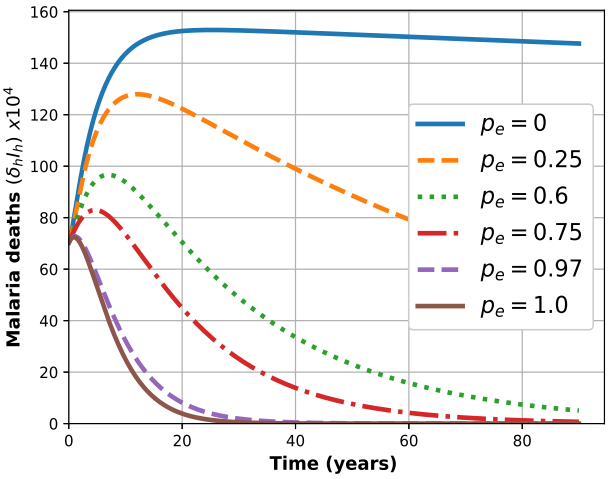

(b) Effect of varying p_e on number of malaria deaths, $\delta_h I_h$

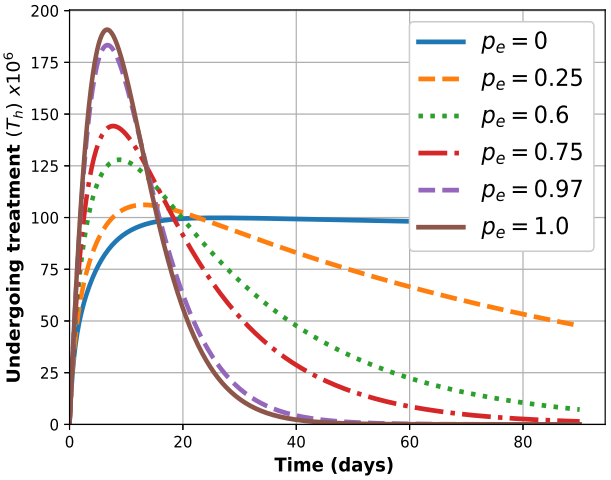

(c) Effect of varying p_e on number of humans undergoing treatment, T_h

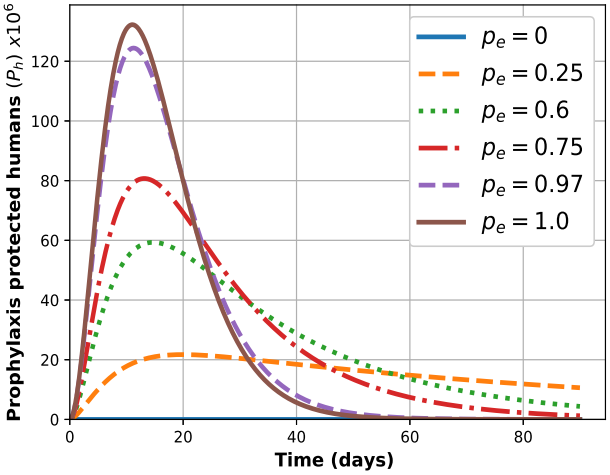

(d) Effect of varying p_e on number of protected after treatment, P_h

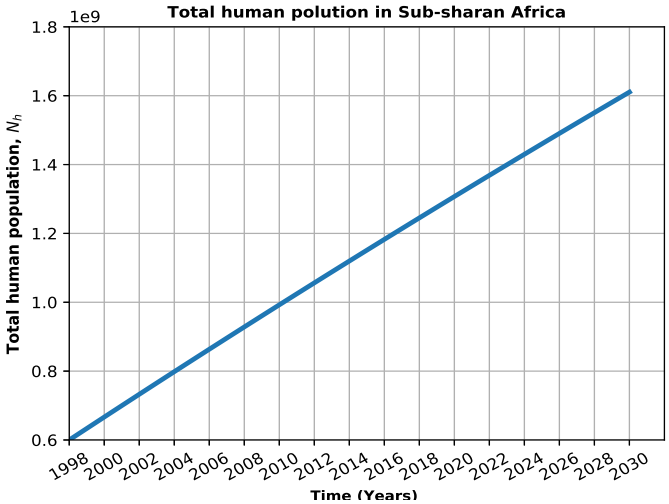

(e) Total human population in Sub-Saharan Africa.

Figure 7: Simulations showing the effect of varying the parameter p_e on the number of infected, taking treatment, protected and malaria caused deaths. All parameter values and initial conditions are the same as in Figure 6 except that we vary p_e between 0 and 1. Here $\alpha_h = 0.35$ fixed. Subfigure 7e shows a simulation of total human population for a fixed $p_e = 0.55$ and $\alpha_h = 0.35$.

5 Discussion and conclusion

One of the current topics in malaria research is to design interventions to block gametocyte transmission to the vectors (female *Anopheles* mosquitoes) or sporozoites transmission to humans, in order to control and eradicate the disease. The main idea is to disrupt the parasites' reproduction and its further development in the mosquito, thus breaking the life cycle of the parasite, [39]. In this paper, we formulated and analyzed a mathematical model for the transmission dynamics of malaria that considers a treatment using a transmission-blocking antimalarial drug (TBD). The formulated model consists of nine compartments. Mathematical and epidemiological implications of the TBDs are assessed using different methods such as determining the effective treatment reproduction number $\mathcal{R}_T$, critical treatment rate $\alpha_h^{\#}$, sensitivity analysis, backward bifurcation analysis and data fitting.

We validated our model by fitting it to real data obtained from the IHME-GBD web-site. We used a non-linear least-squares minimization and curve-fitting package in python known as "lmfit". The fitted curves of the model well reflect the data and agree with the current dynamics of malaria in Sub-Saharan Africa. Together with fitting the state curves, we have also estimated values of the parameters in the malaria model. Our projected model results show that if, in addition to the existing control strategies against malaria, other control measures such as a highly efficacious TBD with high treatment coverage are applied, the number of malaria cases and deaths can be greatly reduced in a few years. Thus, an ultimate goal in an effort to completely eliminate and eradicate malaria is to design a novel transmission-blocking treatment that can cure malaria patients and completely block the formation or maturation of gametocytes so that the malaria parasites will be not passed on.

We believe that our model can provide some insights into the effect of TBDs in terms of malaria transmission control and thus help in the drug development and regulatory decision-making processes, leading to a more affordable and effective drug therapy. The results obtained from our model should be also useful for the development of improved models that can incorporate the clinical drug pharmacokinetics and pharmacodynamic properties.

Acknowledgment

All authors acknowledge the financial support from the DST/NRF SARChI Chair in Mathematical Models and Methods in Biosciences and Bioengineering at the University of Pretoria, grant No. 82770.

Conflict of Interest

All authors declare no potential conflict of interest.

References

1. Aher, R. B. and Roy, K. (2019). Design of antimalarial transmission blocking agents: Pharmacophore mapping of ligands active against stage-v mature gametocytes of *Plasmodium falciparum*. *Journal of Biomolecular Structure and Dynamics*, 37(14):3660–3673. 17

2. Alzahrani, E. O., Ahmad, W., Khan, M. A., and Malebary, S. J. (2020). Optimal control strategies of zika virus model with mutant. *Communications in Nonlinear Science and Numerical Simulation*, 93:105532. 17

3. Anderson, R. M., Anderson, B., and May, R. M. (1992). *Infectious diseases of humans: dynamics and control*. Oxford university press. 2

4. Andrews, K. A., Wesche, D., McCarthy, J., Möhrle, J. J., Tarning, J., Phillips, L., Kern, S., and Grasela, T. (2018). Model-informed drug development for malaria therapeutics. *Annual review of pharmacology and toxicology*, 58:567–582. 2, 3

5. Aron, J. L. and May, R. M. (1982). The population dynamics of malaria. In *The population dynamics of infectious diseases: theory and applications*, pages 139–179. Springer. 2

6. Arrow, K., Peto, R., et al. (2006). *Saving Lives, Buying Time: Economics of Malaria Drugs in an Age of Resistance*. Office of Health Economics. 2

7. Beretta, E., Capasso, V., and Garao, D. G. (2018). A mathematical model for malaria transmission with asymptomatic carriers and two age groups in the human population. *Mathematical biosciences*, 300:87–101. 2

8. Birkhoff, G. and Rota, G. (1989). *Ordinary Differential Equations*. Wiley, fourth edition. 8

9. Birkholtz, L.-M., Coetzer, T. L., Mancama, D., Leroy, D., and Alano, P. (2016). Discovering new transmission-blocking antimalarial compounds: challenges and opportunities. *Trends in parasitology*, 32(9):669–681. 2, 3, 17

10. Bonyah, E., Khan, M. A., Okosun, K., and Islam, S. (2017). A theoretical model for zika virus transmission. *PloS one*, 12(10):e0185540. 9, 17, 29

11. Bonyah, E., Khan, M. A., Okosun, K. O., and Gómez-Aguilar, J. (2019). On the co-infection of dengue fever and zika virus. *Optimal Control Applications and Methods*, 40(3):394–421. 9, 17, 29

12. Bretscher, M. T., Griffin, J. T., Ghani, A. C., and Okell, L. C. (2017). Modelling the benefits of long-acting or transmission-blocking drugs for reducing *Plasmodium falciparum* transmission by case management or by mass treatment. *Malaria journal*, 16(1):341. 3, 12

13. Buonomo, B. and Vargas-De-León, C. (2012). Global stability for an hiv-1 infection model including an eclipse stage of infected cells. *Journal of Mathematical Analysis and Applications*, 385(2):709–720. 17

14. Buonomo, B. and Vargas-De-León, C. (2013). Stability and bifurcation analysis of a vector-bias model of malaria transmission. *Mathematical Biosciences*, 242(1):59–67. 9, 17, 29

15. Burrows, J. N., Duparc, S., Gutteridge, W. E., van Huijsduijnen, R. H., Kaszubska, W., Macintyre, F., Mazzuri, S., Möhrle, J. J., and Wells, T. N. (2017). New developments in anti-malarial target candidate and product profiles. *Malaria journal*, 16(1):26. 2, 17

16. Chitnis, N., Cushing, J. M., and Hyman, J. (2006). Bifurcation analysis of a mathematical model for malaria transmission. *SIAM Journal on Applied Mathematics*, 67(1):24–45. 2, 3, 6, 12

17. Chitnis, N., Hyman, J. M., and Cushing, J. M. (2008). Determining important parameters in the spread of malaria through the sensitivity analysis of a mathematical model. *Bulletin of mathematical biology*, 70(5):1272. 12

18. Chowell, G. (2017). Fitting dynamic models to epidemic outbreaks with quantified uncertainty: a primer for parameter uncertainty, identifiability, and forecasts. *Infectious Disease Modelling*, 2(3):379–398. 18

19. Danbaba, A. et al. (2016). *Mathematical models and analysis for the transmission dynamics of malaria*. PhD thesis, University of Pretoria. 3, 6, 17

20. Danquah, B., Chirove, F., and Banasiak, J. (2019). Effective and ineffective treatment in a malaria model for humans in an endemic region. *Afrika Matematika*, 30(7-8):1181–1204. 2

21. Delves, M., Angrisano, F., and Blagborough, A. (2018). Antimalarial transmission-blocking interventions: past, present, and future. *Trends in parasitology*, 34(9):735–746. 2, 3, 17

22. Diekmann, O., Heesterbeek, J. A. P., and Metz, J. A. (1990). On the definition and the computation of the basic reproduction ratio $\mathcal{R}_0$ in models for infectious diseases in heterogeneous populations. *Journal of mathematical biology*, 28(4):365–382. 9, 28

23. Erdfelder, E., Castela, M., Michalkiewicz, M., and Heck, D. W. (2015). The advantages of model fitting compared to model simulation in research on preference construction. *Frontiers in psychology*, 6:140. 17

24. Filipe, J. A., Riley, E. M., Drakeley, C. J., Sutherland, C. J., and Ghani, A. C. (2007). Determination of the processes driving the acquisition of immunity to malaria using a mathematical transmission model. *PLoS computational biology*, 3(12):e255. 2

25. Forouzannia, F. and Gumel, A. B. (2014). Mathematical analysis of an age-structured model for malaria transmission dynamics. *Mathematical biosciences*, 247:80–94. 2

26. Gething, P. W., Smith, D. L., Patil, A. P., Tatem, A. J., Snow, R. W., and Hay, S. I. (2010). Climate change and the global malaria recession. *Nature*, 465(7296):342–345. 2

27. Global Burden of Disease Collaborative Network (2018). Global burden of disease study 2017 (gbd 2017) results. http://ghdx.healthdata.org/gbd-results-tool. Accessed: 09 May, 2020. 19, 20

28. Golub, G. H. and Van Loan, C. F. (1996). Matrix Computations, Johns Hopkins University Press. *Baltimore and London*. 28

29. Griffin, J. T., Ferguson, N. M., and Ghani, A. C. (2014). Estimates of the changing age-burden of *Plasmodium falciparum* malaria disease in Sub-Saharan Africa. *Nature communications*, 5:3136. 12

30. Gumel, A. (2012). Causes of backward bifurcations in some epidemiological models. *Journal of Mathematical Analysis and Applications*, 395(1):355–365. 15

31. Hancock, P., Thomas, M. B., and Godfray, H. (2009). An age-structured model to evaluate the potential of novel malaria-control interventions: a case study of fungal biopesticide sprays. *Proceedings of the Royal Society B: Biological Sciences*, 276(1654):71–80. 2

32. Hsieh, P.-F. and Sibuya, Y. (2012). *Basic theory of ordinary differential equations*. Springer Science & Business Media. 8

33. Institute for Health Metrics and Evaluation-Global Burden of Disease (2018). Global burden of disease study 2017 (gbd 2017) results. http://ghdx.healthdata.org/gbd-results-tool. Last updated: 2018-12-20, Acessed: 2020-03-23. 17, 18

34. Jiang, J., Qiu, Z., Wu, J., and Zhu, H. (2009). Threshold conditions for west nile virus outbreaks. *Bulletin of mathematical biology*, 71(3):627–647. 15

35. Kamgang, J. C. and Sallet, G. (2005). Global asymptotic stability for the disease free equilibrium for epidemiological models. *Comptes Rendus Mathematique*, 341(7):433–438. 9, 17

36. Kamgang, J. C. and Sallet, G. (2008). Computation of threshold conditions for epidemiological models and global stability of the disease-free equilibrium (dfe). *Mathematical biosciences*, 213(1):1–12. 9

37. Khan, M., Shah, S. W., Ullah, S., and Gómez-Aguilar, J. (2019). A dynamical model of asymptomatic carrier zika virus with optimal control strategies. *Nonlinear Analysis: Real World Applications*, 50:144–170. 9, 17, 29

38. Khanafer, A., Başar, T., and Gharesifard, B. (2016). Stability of epidemic models over directed graphs: A positive systems approach. *Automatica*, 74:126–134. 9

39. Kuehn, A. and Pradel, G. (2010). The coming-out of malaria gametocytes. *BioMed Research International*, 2010. 23

40. Li, M. Y. and Muldowney, J. S. (1996). A geometric approach to global-stability problems. *SIAM Journal on Mathematical Analysis*, 27(4):1070–1083. 17

41. Lindblade, K. A., Steinhardt, L., Samuels, A., Kachur, S. P., and Slutsker, L. (2013). The silent threat: asymptomatic parasitemia and malaria transmission. *Expert review of anti-infective therapy*, 11(6):623–639. 4

42. Macdonald, G. et al. (1957). The epidemiology and control of malaria. *The Epidemiology and Control of Malaria*. 2

43. Martcheva, M. (2015). *An introduction to mathematical epidemiology*, volume 61. Springer. 19

44. Mukhtar, A. Y., Munyakazi, J. B., and Ouifki, R. (2019). Assessing the role of climate factors on malaria transmission dynamics in south sudan. *Mathematical biosciences*, 310:13–23. 2

45. Newville, M., Stensitzki, T., Allen, D. B., Rawlik, M., Ingargiola, A., and Nelson, A. (2016). Lmfit: Non-linear least-square minimization and curve-fitting for python. *Astrophysics Source Code Library*. 3, 18

46. Ngwa, G. A. and Shu, W. S. (2000). A mathematical model for endemic malaria with variable human and mosquito populations. *Mathematical and Computer Modelling*, 32(7-8):747–763. 2, 3, 6, 12

47. Okosun, K. O., Ouifki, R., and Marcus, N. (2011). Optimal control analysis of a malaria disease transmission model that includes treatment and vaccination with waning immunity. *Biosystems*, 106(2-3):136–145. 2

48. Okosun, K. O., Rachid, O., and Marcus, N. (2013). Optimal control strategies and cost-effectiveness analysis of a malaria model. *BioSystems*, 111(2):83–101. 2

49. Okuneye, K., Abdelrazec, A., and Gumel, A. B. (2018). Mathematical analysis of a weather-driven model for the population ecology of mosquitoes. *Mathematical Biosciences & Engineering*, 15(1):57. 2

50. Ouifki, R. and Banasiak, J. (2020). Epidemiological models with quadratic equation for endemic equilibria—a bifurcation atlas. *Mathematical Methods in the Applied Sciences*. 14, 15

51. Peatey, C. L., Skinner-Adams, T. S., Dixon, M. W., McCarthy, J. S., Gardiner, D. L., and Trenholme, K. R. (2009). Effect of antimalarial drugs on *Plasmodium falciparum* gametocytes. *The Journal of infectious diseases*, 200(10):1518–1521. 3

52. Perko, L. (2001). *Differential equations and dynamical systems*, volume 7 of *Texts in Applied Mathematics*. Springer-Verlag, New York, third edition. 8

53. Reluga, T. C., Medlock, J., and Perelson, A. S. (2008). Backward bifurcations and multiple equilibria in epidemic models with structured immunity. *Journal of theoretical biology*, 252(1):155–165. 15

54. Roser, M. and Ritchie, H. (2019). Malaria. *Our World in Data*. https://ourworldindata.org/malaria. 3, 18, 19, 20

55. Ross, R. (1910). *The prevention of malaria*. Dutton. 2

56. Rudrapal, M. (2011). A brief review on malaria and current antimalarial drugs. *Current Pharma Research*, 1(3):286. 2

57. Sinden, R. E. (2017). Developing transmission-blocking strategies for malaria control. *PLoS Pathogens*, 13(7). 2, 3, 17

58. Slater, H. C., Okell, L. C., and Ghani, A. C. (2017). Mathematical modelling to guide drug development for malaria elimination. *Trends in parasitology*, 33(3):175–184. 2, 3

59. Smith, H. L. and Thieme, H. R. (2011). *Dynamical systems and population persistence*, volume 118. American Mathematical Soc. 8

60. The World Bank (2020). Life expectancy at birth, total (years) Sub-Saharan Africa. https://data.worldbank.org/indicator/SP.DYN.LE00.IN?locations=ZG. Accessed: 07 Aug 202020. 19

61. Thota, S. and Yerra, R. (2016). Drug discovery and development of antimalarial agents: recent advances. *Current Protein and Peptide Science*, 17(3):275–279. 2, 17

62. Turányi, T. (1990). Sensitivity analysis of complex kinetic systems. tools and applications. *Journal of mathematical chemistry*, 5(3):203–248. 12

63. United Nations Department of Economic and Social Affairs PopulationDynamics (2020). World population prospects 2019. https://population.un.org/wpp/. Accessed: 07 Aug 202020. 18, 19

64. Van den Driessche, P. and Watmough, J. (2002). Reproduction numbers and sub-threshold endemic equilibria for compartmental models of disease transmission. *Mathematical biosciences*, 180(1):29–48. 9, 28, 29

65. Van den Driessche, P. and Watmough, J. (2008). Further notes on the basic reproduction number. In *Mathematical epidemiology*, pages 159–178. Springer. 9, 17, 29

66. Wadi, I., Anvikar, A. R., Nath, M., Pillai, C. R., Sinha, A., and Valecha, N. (2018). Critical examination of approaches exploited to assess the effectiveness of transmission-blocking drugs for malaria. *Future medicinal chemistry*, 10(22):2619–2639. 2, 3, 17

67. White, L. J., Maude, R. J., Pongtavornpinyo, W., Saralamba, S., Aguas, R., Van Effelterre, T., Day, N. P., and White, N. J. (2009). The role of simple mathematical models in malaria elimination strategy design. *Malaria journal*, 8(1):212. 2

68. Woldegerima, W. A., Ngwa, G. A., and Teboh-Ewungkem, M. I. (2018). Sensitivity analysis for a within-human-host immuno-pathogenesis dynamics of *Plasmodium falciparum* parasites. *Texts in Biomathematics*, 1:140–168. 11, 12

69. World Health Organization (2018). World malaria report 2018e. https://www.who.int/malaria/publications/world-malaria-report-2018/en/. Last update: 19 November 2018. 1

70. World Health Organization (2019). World malaria report 2019. https://www.who.int/publications/i/item/9789241565721. Accessed: 09 May, 2020. 1

71. World Health Organization and others (2018). Overview of malaria treatment. https://www.who.int/malaria/areas/treatment/overview/en/. Last update: 18 January 2018, Accessed: 08 November 2019. 2

72. World Health Organization-Global Health Observatory data repository (2016). Data-malaria. https://apps.who.int/gho/data/node.main.A1362?lang=en. Last updated: 2019-02-12, Acessed: 2020-03-27. 17

73. World Population Review (2020). Sub saharan africa population 2020. https://worldpopulationreview.com/continents/sub-saharan-africa-population. Accessed: 07 Aug 202020. 18, 19

74. Yang, H. M. and Ferreira, M. U. (2000). Assessing the effects of global warming and local social and economic conditions on the malaria transmission. *Revista de saude publica*, 34(3):214–222. 2

75. Zi, Z. (2011). Sensitivity analysis approaches applied to systems biology models. *IET systems biology*, 5(6):336–346. 12

Appendix

Computation of control reproduction number

To calculate the control reproduction number, $\mathcal{R}_T$ for (1), we use the *the next-generation matrix method* based on [22, 64]. For this, let us rewrite system (1) as:

$$\begin{cases} \boldsymbol{x}_d' = \boldsymbol{f}_1(\boldsymbol{x}_d, \boldsymbol{x}_s), \\ \boldsymbol{x}_s' = \boldsymbol{f}_2(\boldsymbol{x}_d, \boldsymbol{x}_s), \end{cases} \tag{31}$$

where $\boldsymbol{x}_d = (E_h,\ I_h,\ T_h,\ R_h,\ E_v,\ I_v)^T$ are the infectious compartments and $\boldsymbol{x}_s = (S_h,\ P_h,\ S_v)^T$ are the disease free ones. Thus, the DFE of system (31) will be

$$\boldsymbol{x}_0^* = (\boldsymbol{x}_d^*, \boldsymbol{x}_s^*) = (E_h^*, I_h^*, T_h^*, R_h^*, E_v^*, I_v^*, S_h^*, P_h^*, S_v^*) = \left(0,\ 0,\ 0,\ 0,\ 0,\ 0,\ \frac{\Pi_h}{\mu_h},\ 0,\ \frac{\Pi_v}{\mu_v}\right).$$

We recall that to determine the control reproduction number, due to the Schur factorization, it is sufficient to use only the diseased (infected) compartments, see [64, Lemma 1] and [28, Section 7.7]. So, using the system for $\boldsymbol{x}_d'$, let $\mathcal{F}_i$ be the rate of appearance of new infections in the compartment i, $\mathcal{V}_i^-$ be the rate of transfer of individuals out of the compartment i by all other means and $\mathcal{V}_i^+$ be the rate of transfer of individuals into the compartment i by all other means. Set $\mathcal{V}_i = \mathcal{V}_i^- - \mathcal{V}_i^+$ and $\mathcal{F} = [\mathcal{F}_i]\,,\quad \mathcal{V} = [\mathcal{V}_i]\,,\quad i = 1, 2, \cdots, 6$ and hence

$$\mathcal{F} = \begin{pmatrix} \frac{I_v S_h b \beta_{vh}}{E_h+I_h+P_h+R_h+S_h+T_h} \\ 0 \\ 0 \\ 0 \\ \frac{(E_h\zeta_e+R_h\zeta_r+T_h\zeta_t+I_h)S_v b\beta_{hv}}{E_h+I_h+P_h+R_h+S_h+T_h} \\ 0 \end{pmatrix},\ \mathcal{V} = \begin{pmatrix} E_h(\mu_h+\nu_h) \\ (\Gamma_4+\alpha_h)I_h - \Gamma_1 T_h - E_h\nu_h \\ (\Gamma_1+\Gamma_2+\Gamma_3+\mu_h)T_h - I_h\alpha_h \\ -\Gamma_2 T_h - I_h\gamma_h + R_h(\mu_h+\rho_h) \\ E_v(\mu_v+\nu_v) \\ I_v\mu_v - E_v\nu_v \end{pmatrix}. \tag{32}$$

Then their corresponding Jacobian matrices, F and V, respectively, evaluated at the DFE $\boldsymbol{x}_0^*$ are,

$$F = \left[\frac{\partial \mathcal{F}_i}{\partial x_j}(\boldsymbol{x}_0^*)\right] = \begin{bmatrix} 0 & 0 & 0 & 0 & 0 & b\beta_v \\ 0 & 0 & 0 & 0 & 0 & 0 \\ 0 & 0 & 0 & 0 & 0 & 0 \\ 0 & 0 & 0 & 0 & 0 & 0 \\ \Gamma_6\zeta_e & \Gamma_6 & \Gamma_6\zeta_t & \Gamma_6\zeta_r & 0 & 0 \\ 0 & 0 & 0 & 0 & 0 & 0 \end{bmatrix} \text{ and}$$

$$V = \left[\frac{\partial \mathcal{V}_i}{\partial x_j}(\boldsymbol{x}_0^*)\right] = \begin{bmatrix} \mu_h+\nu_h & 0 & 0 & 0 & 0 & 0 \\ -\nu_h & \Gamma_4+\alpha_h & -\Gamma_1 & 0 & 0 & 0 \\ 0 & -\alpha_h & \Gamma_1+\Gamma_5 & 0 & 0 & 0 \\ 0 & -\gamma_h & -\Gamma_2 & \mu_h+\rho_h & 0 & 0 \\ 0 & 0 & 0 & 0 & \mu_v+\nu_v & 0 \\ 0 & 0 & 0 & 0 & -\nu_v & \mu_v \end{bmatrix},$$

where

$$\omega_h := q_h\theta_h,\ \sigma_h := (1-q_h)\theta_h,\ \Gamma_1 := (1-p_e)\omega_h,\ \ \Gamma_2 := (1-p_e)\sigma_h,\ \ \Gamma_3 := p_e r_h,$$

$$\Gamma_4 := \delta_h + \gamma_h + \mu_h,\ \ \Gamma_5 := \Gamma_2 + \Gamma_3 + \mu_h,\ \ \Gamma_6 := \frac{\Pi_v b\beta_{hv}\mu_h}{\Pi_h\mu_v},\ \ \Gamma_7 := \Gamma_1 + \Gamma_5.$$

Thus, the control reproduction number, $\mathcal{R}_T$, which is the spectral radius of the next generation matrix, $G = FV^{-1}$ is computed to be:

$$\mathcal{R}_T = \sqrt{\frac{\Gamma_6 b\beta_{vh}\nu_v\left[\nu_h(\mu_h+\rho_h)\left(\Gamma_7+\alpha_h\zeta_t\right)+\left(\Gamma_2\alpha_h+(\Gamma_7)\gamma_h\right)\nu_h\zeta_r+\zeta_e\Big(\Gamma_4\Gamma_7+\Gamma_5\alpha_h\Big)\Big(\mu_h+\rho_h\Big)\right]}{\left(\Gamma_4\Gamma_7+(\Gamma_5\alpha_h)\right)(\mu_h+\nu_h)\left(\mu_h+\rho_h\right)(\mu_v+\nu_v)\,\mu_v}}.$$

This can be written as

$$\mathcal{R}_T^2 = \mathcal{R}_0^2\xi\left(\alpha_h\right),$$

where $\mathcal{R}_0$ and $\xi\left(\alpha_h\right)$ was defined in (14). □

Proof of Theorem 2 (locally stability of DFE)

Here we show that the DFE of model (1) is locally asymptotically stable. The proof follows the lines of [64, Theorem 2] and [65, Lemma 2]. To simplify the notation, we write:

$x_i \in (E_h, I_h, T_h, R_h, E_v, I_v, S_h, P_h, S_v), i = 1, 2, \cdots, 9$, $x_{di} \in (E_h,\ I_h,\ T_h,\ R_h,\ E_v,\ I_v),\ i = 1, 2, \cdots, 6$ and $x_{si} \in (S_h, P_h, S_v),\ i = 7, 8, 9$.

(A1) Clearly from (32), we can easily observe that if $\boldsymbol{x} \geq 0$, then each $\mathcal{F}_i,\ \mathcal{V}_i^+,\ \mathcal{V}_i^- \geq 0$ for each $i = 1, ..., 9$, where the inequalities are entry-wise.

(A2) If a compartment is empty, then there is no transfer out of that compartment. Let any state variable, $x_i \in (E_h,\ I_h,\ T_h,\ R_h,\ E_v,\ I_v,\ S_h,\ P_h,\ S_v)$ be zero. Then, from (32), it is obvious that $\mathcal{V}_i^- = 0$. In particular, if $x_i \in \boldsymbol{x}_s$, then $\mathcal{V}_i^- = 0$. We already have showed that the system (31) has a non negative, bounded and unique solution provided that the initial data is positive.

(A3) From (32), we can see that $\mathcal{F}_7 = 0 = \mathcal{F}_8 = \mathcal{F}_9$. That is, $\mathcal{F}_i = 0$, for $i > 6$. Thus, the incidence of infection for uninfected compartments $(S_h,\ P_h, S_v)$ is zero.

(A4) We can easily observe from (32) that if $\boldsymbol{x} \in \boldsymbol{x}_s$, then we have $\mathcal{F}_i = 0$ and $\mathcal{V}_i = 0$ for $i = 1, \cdots, 6$. Furthermore, the corresponding disease-free subsystem

$$\frac{dS_h}{dt} = \Pi_h - \mu_h S_h, \tag{33}$$

$$\frac{dS_v}{dt} = \Pi_v - \mu_v S_v. \tag{34}$$

has an equilibrium point $(\frac{\Pi_h}{\mu_h},\ \frac{\Pi_v}{\mu_v})$ which is globally asymptotically stable.

(A5) For the diseased (infected) subsystem, that is, for $1 \leq i,\ j \leq 6$, we have the matrices given in (33) and (33). Thus, we observe that matrix F is non-negative. The determinant of V is $det(\tilde{V}) = \mu_v(\mu_v+\nu_v)(\mu_h+\rho_h)(\mu_h+\nu_h)\Big(\Gamma_5(\Gamma_4+\alpha_h)-\Gamma_1\alpha_h\Big)$. But, $\Gamma_5(\Gamma_4+\alpha_h)-\Gamma_1\alpha_h = \Gamma_5\Gamma_4+\Gamma_5\alpha_h-\Gamma_1\alpha_h = \Gamma_5\Gamma_4+\alpha_h(\Gamma_2+\Gamma_3+\mu_h) > 0$. Hence, the matrix V is non-singular. We can also easily see that V is an M-matrix. Hence, by [65, Lemma 2], all eigenvalues of $F - V$ have negative real parts. Therefore, by [64, Theorem 2] and [65, Theorem 1], the DFE $\boldsymbol{x}_0^*$ of system (1) is locally asymptotically stable if $\mathcal{R}_T < 1$, but unstable if $\mathcal{R}_T > 1$. □

We note that the local stability of the DFE can also be proved by determining condition for which all eigenvalues of the model at the DFE have negative real parts, see for e.g. [10, 11, 14, 37].

Some coefficients determining the occurrence of backward bifurcation

To simplify notations, during the computations of the endemic equilibria and the backward bifurcation analysis, we set

$$\begin{aligned}
K_1 &= \Gamma_5+\Gamma_1,\ K_2=\vartheta+\mu_h,\ K_3=\nu_h+\mu_h,\ K_4=\alpha_h+\Gamma_4,\ K_5=\rho_h+\mu_h,\\
K_6 &= \gamma_h(\Gamma_5+\Gamma_1)+\Gamma_2\alpha_h,\ K_7=\nu_v+\mu_v, C_{vh}=\beta_{vh}b,\ C_{hv}=\beta_{hv}b,\\
C_0 &= \beta_{vh}b\Big(\frac{\zeta_e\Gamma_5(\alpha_h+\Gamma_4)}{\nu_h(\Gamma_5+\Gamma_1)}+\frac{\zeta_t\alpha_h}{(\Gamma_5+\Gamma_1)}+\frac{\zeta_r(\gamma_h(\Gamma_5+\Gamma_1)+\Gamma_2\alpha_h)}{(\rho_h+\mu_h)(\Gamma_5+\Gamma_1)}+1\Big)\\
&= C_{vh}\left(\frac{\zeta_e\Gamma_5K_4}{\nu_hK_1}+\frac{\zeta_t\alpha_h}{K_1}+\frac{\zeta_rK_6}{K_5K_1}+1\right),\\
K_0 &= \frac{\nu_v\Pi_v}{\mu_v(\nu_v+\mu_v)}.
\end{aligned}$$

and

$$D_{00}=K_5K_2K_3\Gamma_5K_4,\quad D_{01}=K_2\nu_h\rho_hK_6+K_5\nu_h\vartheta\alpha_h\Gamma_3,\quad D_{02}=\mu_hK_5K_2K_3\Gamma_5K_4=\mu_hD_{00}.$$

Furthermore, we set

$$\begin{aligned}
&\phi_1=K_3\Gamma_5K_4\Pi_hK_5K_2,\ \phi_2=\Gamma_5K_4\Pi_hK_5K_2,\quad \phi_3=\Pi_hK_5K_2K_1\nu_h,\quad \phi_4=\alpha_h\Pi_hK_5K_2\nu_h,\\
&\phi_5=\alpha_h\Gamma_3\Pi_hK_5\nu_h,\quad \phi_6=K_6\Pi_hK_2\nu_h,\quad \phi_7=\phi_2+\cdots+\phi_6,\\
&\phi_8:=\zeta_e\phi_2+\phi_3+\zeta_t\phi_4+\zeta_r\phi_6.
\end{aligned}$$